MAGNETIC PROPERTIES OF THE BOULDER BATHOLITH NEAR HELENA, MONTANA, AND THEIR USE IN MAGNETIC INTERPRETATION

Thesis for the Degree of M. S. MICHIGAN STATE UNIVERSITY INNAIAH POTHACAMURY 1970

1 HESIS

3 1293 10474 5447

LIBRARY

Michigan State

University

ABSTRACT

MAGNETIC PROPERTIES OF THE BOULDER BATHOLITH NEAR HELENA, MONTANA, AND THEIR USE IN MAGNETIC INTERPRETATION

By

Innaiah Pothacamury

Magnetic rock properties of samples from the two major rock types of the Boulder Batholith have been measured. Fifteen of the sites are from the marginal Unionville granodiorite at the northern end of the batholith, and 18 sites are from the interior Clancy granodiorite. The samples from all the sites were a.f. demagnetized at 125 cersteds to eliminate secondary components of remanent magnetization. Data from samples from 6 sites in the Unionville granodiorite and 11 sites from the Clancy granodiorite which had circles of confidence of 30° or less were used in the calculation of rock type averages.

The average intensity of NRM of samples from 6 sites in the Unionville granodiorite was 570×10^{-6} emu per cc, the inclination was 63.2° and the declination was 39.4° . The samples from 11 sites in the Clancy granodiorite had an average intensity of NRM of 390×10^{-6} emu per cc, an inclination of 64.0° and a declination of 347.8° . These were the average values used in modeling studies, and were obtained after a.f. demagnetization at 125 cersteds.

The average magnetic susceptibility of samples from Unionville granodiorite was 2730x10⁻⁶ emu per cc, and the

average susceptibility of samples from the Clancy granodiorite was 2510x10⁻⁶ emu per cc. The susceptibility of samples from sites in the Clancy granodiorite decreased linearly with respect to the distance from the intrusive contact. Comparison of calculated magnetic profiles with an observed magnetic profile suggested that the magnetic susceptibility contrasts of the Unionville granodiorite and Clancy granodiorite with the intruded rocks are 2500x10⁻⁶ and 2000x10⁻⁶ emu per cc respectively. The difference between these susceptibility contrasts and the measured susceptibilities is believed to be a result of lower average susceptibility within the rock units due to alteration and the low magnetic susceptibility of the intruded rocks. the modeling studies the Clancy granodiorite also was divided into eight discrete bodies with decreasing susceptibility with increasing distance from the intrusive contact.

Theoretical magnetic profiles were obtained with various body configurations and compared with an observed profile. The calculated profile that had a reasonably good fit with the observed magnetic profile had vertical contacts to the bottom of the batholith which was assumed to lie at a depth of 10 km, after dipping to the northeast to a depth of 2.6 km. The magnetic polarization was induced plus remanent. The profiles obtained with induced magnetization only did not match the observed profile.

The model proposed in this study is different from a model previously proposed on the basis of gravity data.

The difference is explained in terms of the density values used in obtaining the gravity model.

MAGNETIC PROPERTIES OF THE BOULDER BATHOLITH NEAR HELENA, MONTANA, AND THEIR USE IN MAGNETIC INTERPRETATION

В**у**

Innaiah Pothacamury

A THESIS

Submitted to
Michigan State University
in partial fulfillment of the requirements
for the degree of

MASTER OF SCIENCE

Department of Geology

1970

ACKNOWLEDGMENTS

The author wishes to acknowledge his gratitude to Dr. W. J. Hinze for his guidance, advice, and understanding throughout the course of this study.

The author is also grateful to D. D. Sanderson for collecting the samples used in this study, and for assistance throughout this study. The author is thankful to Dr. J. W. Trow and Dr. H. B. Stonehouse for reviewing the thesis, and to T. W. MacClure for help with the spinner magnetometer.

TABLE OF CONTENTS

LIST	OF	TABLES	Page iv
LIST	OF	'FIGURES	. A
Chapt	ter	•	
•	ī.	INTRODUCTION	1
I:	ı.	GEOLOGY OF THE BOULDER BATHOLITH	5
II	ı.	REVIEW OF GEOPHYSICAL STUDIES OF THE BATHOLITH	10
I	٧.	THE SPINNER MAGNETOMETER	14
1	٧.	MEASURED MAGNETIC ROCK PROPERTIES	21
V:	I.	MAGNETIC MODELS OF THE NORTHERN MARGIN OF THE BATHOLITH	44
VI	ı.	SUMMARY	59
T.T.ST	OF	REFERENCES	62

LIST OF TABLES

[able		Page
1.	Analysis of Plutonic Rocks of the Boulder Batholith	6
2.	Measured Properties of the Unionville Granodiorite	24
3.	Measured Properties of the Clancy Grano-diorite	26

LIST OF FIGURES

Figure		Page
1.	Generalized geologic map of area	2
2.	Angular relationships in the double spin procedure	15
3.	Identification of rock sample magnetic components	15
4.	Block diagram of spinner magnetometer	17
5.	Schematic diagram of phase shifter, attenuator and mixer circuits	19
6.	Equal area projection for samples from site UN-1	28
7.	Equal area projection for samples from site UN-3	28
₽.	Equal area projection for samples from site UN=4	29
9•	Equal area projection for samples from site UN-5	29
10.	Equal area projection for samples from site UN-6	30

Figure			Page
11.	Equal area projection for samples from site UN-7	•	30
12.	Equal area projection for samples from site CL-2	•	31
13.	Equal area projection for samples from site CL-3	•	31
14.	Equal area projection for samples from site CL-5	•	32
15.	Equal area projection for samples from site CL-7	•	32
16.	Equal area projection for samples from site CL-8	•	33
17.	Equal area projection for samples from site CL-10	•	33
18.	Equal area projection for samples from site CL-ll	•	34
19.	Equal area projection for samples from site CL-12	•	34

Figure		Page
20.	Equal area projection for samples from site CL-13	35
21.	Equal area projection for samples from site CL-14	35
22.	Equal area projection for samples from site CL-16	36
23.	Equal area projection for samples from site HC-6	36
24.	Equal area projection for samples from site HC-10	37
25.	Relationship between magnetic susceptibility of Clancy granodiorite and distance from intrusive contact	39
26.	Observed and calculated gravity profile and associated geological model (after Renick, 1965)	45
274.	Portion of the U.S.G.S. aeromagnetic map (GP-538) showing position of analyzed magnetic profile	46
27b.	Location of sample sites with respect to the analyzed magnetic profile	47
28.	Calculated and observed profiles and associated magnetic models derived from gravity studies	52
29.	Calculated and observed profiles and associated magnetic models based on gravity derived model	54

Figure		Pa	age
30a.	Calculated magnetic profiles and associated magnetic models which approximate the observed magnetic profile: Clancy granodiorite assumed to be a single body	•	56
30ъ.	Calculated magnetic profiles and associated magnetic models which approximate the observed magnetic profile: Clancy granodiorite divided into 8 discrete bodies.	•	57

CHAPTER I

INTRODUCTION

The Boulder Batholith is a large plutonic mass exposed throughout some 2200 square miles in southwestern Montana. It extends from Helena 70 miles southward to a little south of Silver Star and is from 25 to 30 miles wide in most places. The exposed part of the batholith is roughly oval shaped and elongate in the north-northeast direction. The east margin is straight and steep for most of its length. The north, south, and west margins are irregular.

Figure 1 after Klepper (1962) is a generalized geologic map of the area, and also shows the location of the area with respect to the State of Montana.

The batholith intrudes rocks ranging in age from Precambrian to late Cretaceous. The age of the batholith is established as very late Cretaceous to early Paleocene based on geologic and geochronometric evidence. The batholith is of a composite nature and is composed of quartz diorite, granodiorite, quartz monzonite, granite, alaskite, aplite, and pegmatite. Approximately 90 percent of the exposed rocks are quartz monzonite or granodiorite. More than two-thirds of the exposed part constitutes a single large body, the Butte quartz monzonite, which is

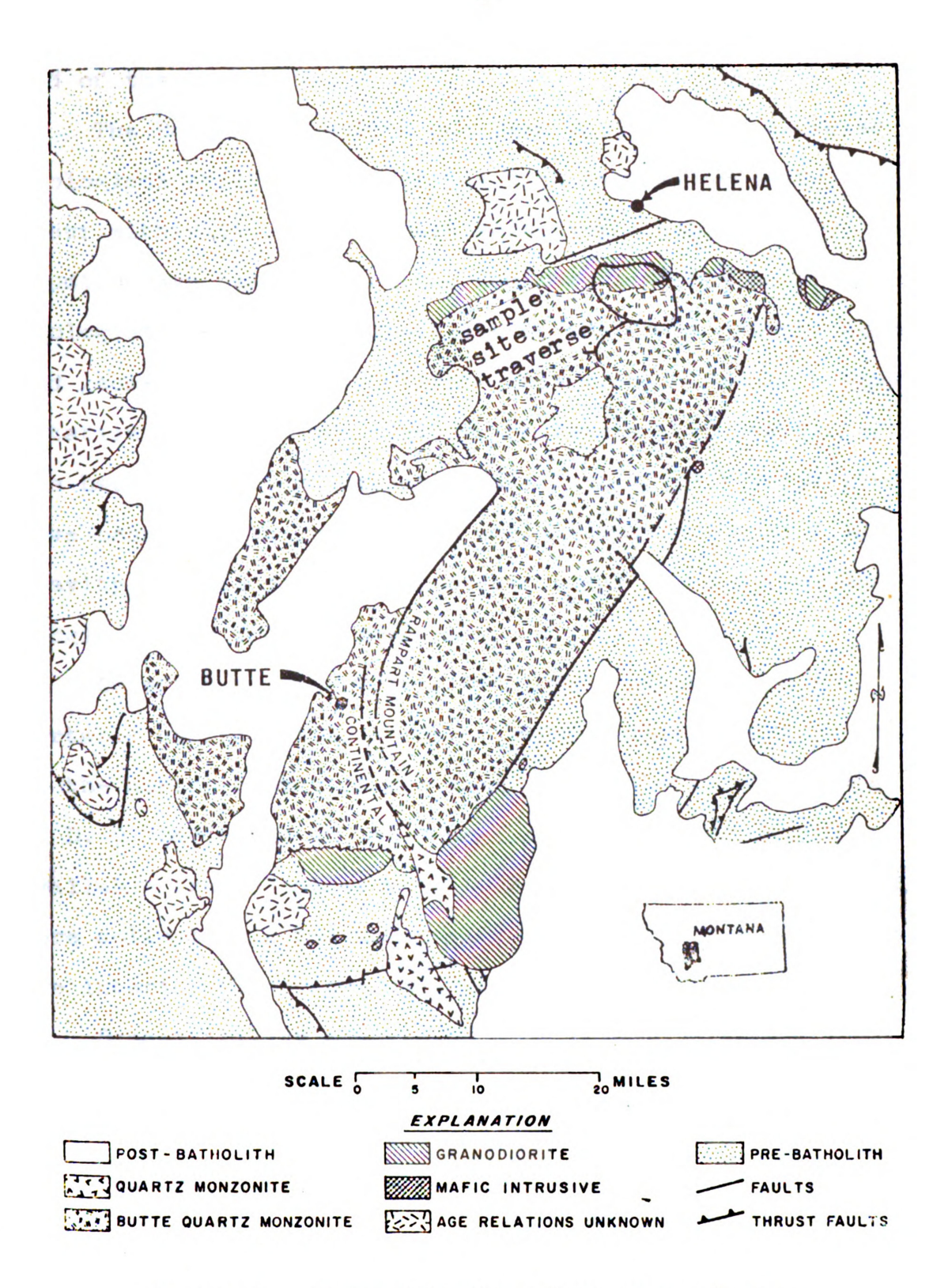


Figure 1. Generalized geologic map of area (After Klepper, 1902)

indistinguishable from the Clancy granodiorite at the northern end of the batholith.

The Boulder Batholith has been subjected to detailed geological study because of the rich mineral deposits which occur within it. In the past seven years geophysical studies have been made on the Boulder Batholith to aid geologists in the interpretation of the areal extent, depth, and geometry of the batholith. This study attempts a quantitative magnetic investigation of the northern margin of the batholith. Rock magnetic data determined from samples have been used in conjunction with available magnetic and gravity data to develop a geologic model for the northern margin of the Boulder Batholith.

Oriented surface rock cores were collected using a portable coring drill, along a traverse approximately normal to the northern part of the Boulder Batholith near Helena, by D. D. Sanderson in the summer of 1968. Samples are available from 33 sites with 6 to 8 samples per site. They were collected in the marginal Unionville granodiorite, and the interior Clancy granodiorite.

Susceptibility measurements were made on all the samples using a susceptibility bridge, and the Q factor, i.e., Koenigsberger ratio was determined for all the sites.

The NRM, i.e., the natural remanent magnetization of a rock is permanent in contrast to the induced magnetization which is temporary and depends on a supporting magnetic field. Several processes are recognized by which rocks

may acquire NRM. The type of NRM acquired by a rock is dependent upon the formation processes and subsequent geologic and magnetic history of the rock.

Measurements of direction and intensity of NRM were made using a spinner magnetometer constructed at the Geology Department of MSU by MacClure (1970) after a design by Doell and Cox (1965). The magnetometer measurements were reduced and plotted by a CDC 3600 computer using a program written by Gromme of the U.S. Geological Survey (private communication) and modified by D. D. Sanderson. The mean direction for each site from the samples of a site was obtained using a method described by Fisher (1953).

To test the stability of the NRM of the samples and to eliminate the secondary components of magnetization, samples from all the 33 sites were a.f. demagnetized in alternating fields using equipment described by Doell and Cox (1967). Samples from 17 sites were a.f. demagnetized at four levels 50, 125, 250 and 400 oersteds. On the basis of the results from these measurements the samples from the remaining 16 sites were a.f. demagnetized only at 125 oersteds.

CHAPTER II

GEOLOGY OF THE BOULDER BATHOLITH

The Boulder Batholith is a composite pluton consisting of quartz diorite, granodiorite, quartz monzonite, granite, alaskite, aplite, and pegmatite. Quartz monozite is by far the most abundant rock type. The rocks intruded by the Boulder Batholith range in age from Beltian (Precambrian) to late Cretaceous.

The order of intrusion of the Boulder Batholith is:

1) Unionville granodiorite, 2) Clancy granodiorite, 3)

phorphyritic granodiorite, 4) biotite adamellite, and 5)

muscovite-biotite granite. Alaskite and aplite are abundant

and were presumably developed most abundantly during the

final stages of bathylithic consolidation. The order of

emplacement of the successive intrusives is in the order

of increasing silica content.

The earliest major intrusive is a granodiorite well exposed south and southeast of Helena. It is dark, and heavy and resembles a diorite. The name Unionville granodiorite has been given to it, after a village four miles south of Helena. It is an augite-biotite-hornblende granodiorite, generally containing some hypersthene.

Table 1: Analysis of Plutonic Rocks of the Boulder Batholith (after Knopf, 1957).

S10 ₂	I 61.14	11 61.40	III 54.63	IV 65.49	V 66.14	VI 71.28	VII 68.48
A12 ⁰ 3	15.28	15.41	16.60	14.49	15.69	14.50	14.93
Fe ₂ 0 ₃	1.90	2.26	3.32	2.11	1.93	1.04	1.32
Fe0	4.52	3.76	5.62	2.90	2.06	1.19	2.07
MgO	3.41	2.99	4.65	2.45	1.60	0.98	1.37
CaO	5.51	4.86	7.93	4.29	3.71	2.45	2.61
Na ₂ 0	2.78	2.69	2.48	2.80	3.50	3.16	3.01
K ₂ 0	3.34	4.12	2.10	3.66	3.54	4.29	4.59

- I: Unionville granodiorite; type locality old quarry NW of BM4589, Clark Gulch. Analyst, J. J. Engel.
- II: Unionville granodiorite; near Benson Xenolith. Analyst, Doris Thaemlitz.
- III: Granogabbro: Analyst, Doris Tahemlitz.
 - IV: Clancy granodiorite: Kain Quarry, Clancy Creek, Analyst, J. J. Engel.
 - V: Porphyritic granodiorite: Analyst, Doris Thaemlitz.
 - VI: Biotite adamellite: Ridge between Jackson Creek and Lump Gulch. Analyst, J. J. Engel.
- VII: Biotite adamellite: Broadwater stock, Helena. Analysts, B. Smith, and R. B. Ellestad.

The second intrusive is the Clancy granodiorite so named from the Kain quarry in Clancy creek which is less than a mile west of Clancy, a town 12 miles southeast of Helena. It is a coarse grained hornblende-biotite granodiorite in which quartz is conspicuous. It is light grey in contrast to the dark grey of the Unionville granodiorite. It is believed that little time elapsed between the intrusion of these two plutons.

Two K-Ar age determinations (Knopf, 1963) have been made on the biotite of the Clancy granodiorite giving an average of 81.5 million years, which means that the intrusion took place in very late Cretaceous time. The Clancy granodiorite is similar to the Butte quartz monzonite in density, appearance and chemical composition.

of the 33 sites at which samples were collected for magnetic rock property study, 15 sites are in the Unionville granodiorite and 18 sites are in the Clancy granodiorite.

Klepper (1962) has dealt in some detail on the mode of emplacement of the batholith. The configuration of the batholith, its relationship to local structural elements, and its internal features provide evidence relating to the mode of emplacement. Basically four mechanisms have been proposed by geologists to account for the emplacement of large intrusive bodies. First is granitization, second, stoping accompanied by assimilation or foundering of the stoped material, third, shouldering aside or mechanically agressive emplacement, and fourth, zone melting. Some

geologists have proposed a combination of some of these processes in attempting to account for large intrusive masses. The amount of granitization and zone melting in the Boulder Batholith is negligible, therefore, these two processes are not considered applicable to this batholith by geologists.

The evidence gathered by many geologists indicates that shouldering aside has taken place at some places, and at some other places evidence shows that stoping has been effective, at least locally. Accordingly workers have reached different conclusions about the mode of emplacement of the Boulder Batholith. Klepper (1962) suggests that shouldering aside was more effective than stoping and assimilation.

According to Klepper (1962), the presence and local abundance of recrystallised inclusions especially in Butte-Clancy rocks indicates that stoping was more than a local phenomenon. Inclusions are relatively abundant in some plutons of the batholith, and sparse or almost absent in others except in the immediate vicinity of the contact. At some places along and near the pluton margins inclusions are large, as much as hundreds of feet across and abundant. At distances more than several hundred feet from most contacts, however, inclusions are small and scattered and of uncertain percentage. These and similar relations suggest that stoping has taken place, but they do not indicate the relative importance of stoping versus shouldering aside.

Klepper (1962) also observed that the pre-batholithic faults exerted a powerful control on the emplacement of the batholith. Structures in the rocks surrounding the batholith also provide a clue to its emplacement. The invaded rocks wrap around the north and south ends of the batholith almost at right angles to the prevailing northerly trend of structures throughout this part of the Rocky Mountain province. These features suggest that shouldering aside was substantial and not merely a local phenomenon in the immediate vicinity of the contact.

According to Tilling and others (1968), the time span of emplacement of the Boulder Batholith is believed to be 7 to 9 million years, with the bulk of the batholith emplaced during the first 6 million years.

CHAPTER III

REVIEW OF GEOPHYSICAL STUDIES OF THE BATHOLITH

Regional gravity surveys have been used to delimit the configuration and depth extent of the batholith. Regional gravity studies of the Boulder Batholith have been made by Biehler and Bonini (1969), Burfeind (1967) and Renick (1965). Renick's study is limited to the northern contact of the batholith. The U.S. Geologic Survey conducted aeromagnetic and gravity studies near the Boulder Batholith, and they have been reported by Pavis and others (1963, 1965a, and 1965b) and Kinoshita and others (1964a, 1964b). A U.S. Geological Survey aeromagnetic map of the Boulder Batholith (GP-538) by Johnson (1965) is also available. Hanna (1967) has reported on the magnetic rock properties of the Elkhorn volcanics. Hanna (1969) also studied the negative aeromagnetic anomalies over mineralized areas of the Boulder Batholith.

Batholiths have been thought by some geologists as large masses of igneous rocks virtually bottomless, i.e., extending to great depths. Many shapes have been postulated for the Boulder Batholith. Biehler and Bonini (1969) observed that the eastern, northern and north-eastern limits of the Boulder Batholith are well defined by steep gravity

gradients which parallel the outcrop of the batholith. general, areas of broad gravity minima are associated with extensive outcrops of the Boulder Batholith and broad gravity maxima are found over pre-batholithic rocks and Precambrian basement. A minimum residual anomaly of -45 milligals is located over the northern end of the batholith. This low then increases to -43 milligals toward the southwest and remains approximately constant throughout the entire length of the intrusive body. This suggests that the intrusive mass has a constant depth throughout the major portion of the axis of the batholith. The western and southwestern extent of this gravity low is indefinite suggesting to Burfeind that the intrusive rocks underlie a considerable area to the west and southwest of the outcrop of the intrusive. Further evidence suggested that the greatest thickness of the intrusive is found along the axis of the gravity low and within the outcrop limits of the main plutonic mass. The northern contact of the main batholithic mass coincides with the steepest gravity gradients of the Bouguer gravity anomaly. Biehler and Bonini (1969) suggest that because of these steep gravity gradients, it is unlikely that any great mass of batholithic rocks extend beyond the northern limit of the present outcrop, and that the contact is steeply dipping.

On the basis of their investigations they calculated the gravitational effect of numerous geologic cross-sections to determine the configuration of the Boulder Batholith. For their calculations they assumed that: 1) the density of the Boulder Batholith is constant with depth, and that the anomaly is caused by density contrasts between the batholithic material and the surrounding rocks; 2) no local warping of the moho is involved, and 3) that the Boulder Batholith can be approximated by a two dimensional body. They tested many batholithic shapes and came up with six configurations which produce anomalies approximately equal to the observed residual anomaly along a profile perpendicular to the long axis of the batholith. However, they do not select any particular configuration as being representative of the Boulder Batholith because of the ambiguity in the interpretation of gravity data. As a result of their studies they suggest that the greatest thickness of the batholithic material is located along the axis of the batholith, with the maximum depth less than 15 km, and probably less than 10 km, possibly 8 km. The floor of the batholith is concave upwards, and is roughly symmetrical in the northern portion. The northwestern and the southeastern margins are shallow, approximately 15°. The northern contact of the batholith is interpreted as steeply dipping to the south.

Burfiend (1967) conducted a gravity survey of the Boulder Batholith and adjacent areas in southwestern Montana. Included in his study was an attempt to determine the subsurface shape and lateral extent of the Boulder Batholith. On the basis of his data he interpreted the Boulder

Batholith to be a tabular body that dips at a low angle to the northwest to approximately -28,000 feet. The northeast contact of the batholith is interpreted to dip to the southwest at about 45° and bottoms at -30,000 feet. At these depths it is believed that they join an extensive pluton of which the Boulder Batholith is an off-shoot. Poorly defined gravity gradients along the southwest margin suggest the lack of a sharp structural delineation between the rocks of the Boulder Batholith and the Idaho Batholith.

The shape of the Boulder Batholith proposed by Burfiend (1967) and Biehler and Bonini (1969) is in sharp contrast to the shapes commonly postulated for batholiths where they are pictured as commonly enlarging downwards, i.e., with the contacts dipping outwards, and the floors at great depths.

Renick (1965) conducted a gravity survey of the Boulder Batholith near Helena, Montana. On the basis of his study he concluded that the batholith has an average thickness of 10,000 feet in the area of his study and that the contact of the batholith with the surrounding sediments dip at 45° to the northeast from the surface to a depth of 3500 feet above sea level, where the dip then reverses to 68° southwest.

Hanna (1969) reports an average susceptibility of 2500x10⁻⁶ emu/cc, and a remanent intensity of about 500x10⁻⁶ emu per cc, for about 600 specimens collected from more than 25 sites in the Boulder Batholith area. However, he provides no further details.

CHAPTER IV

THE SPINNER MAGNETOMETER

The surface core samples collected in the field were cut into samples 2.28 cm in length and 2.49 cm in diameter. The declination, inclination, and intensity of NRM of all the samples were determined using a spinner magnetometer. This magnetometer was constructed by MacClure (1970) after a design by Doell and Cox (1965).

The spinner magnetometer operates on the principle of an alternating current generator in which the magnetic field about a rotating rock sample induces a voltage in a stationary pick up coil assembly. This voltage is amplified and compared to a reference signal of known phase and amplitude for measurement of the phase and intensity of the magnetic component of the rock sample perpendicular to its axis of rotation.

The direction and intensity of NRM are obtained from six spins, i.e., two each about three orthogonal axes, x, y, and z. The z axis is the cylinder axis, y is horizontal in the field orientation, and x is normal to y. Figure 2 shows the first pair of spins. If the component of magnetization normal to the z-axis lies at an angle & from the x axis (measured clockwise towards the y-axis), then ideally the

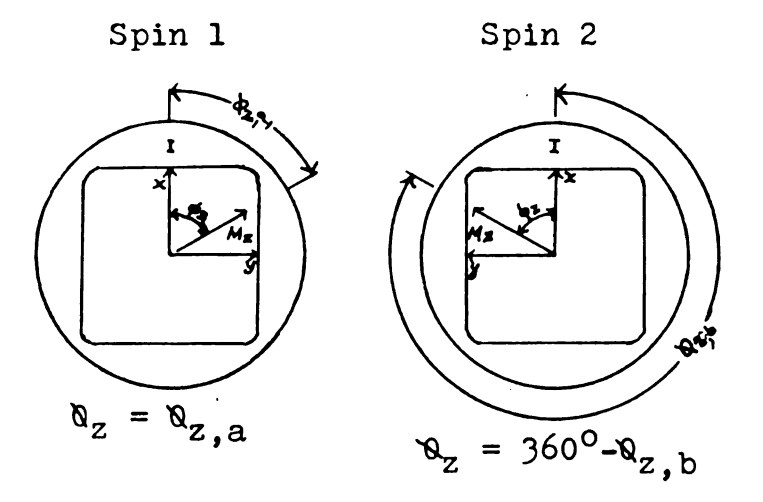


Figure 2. Angular relationships in the double spin procedure

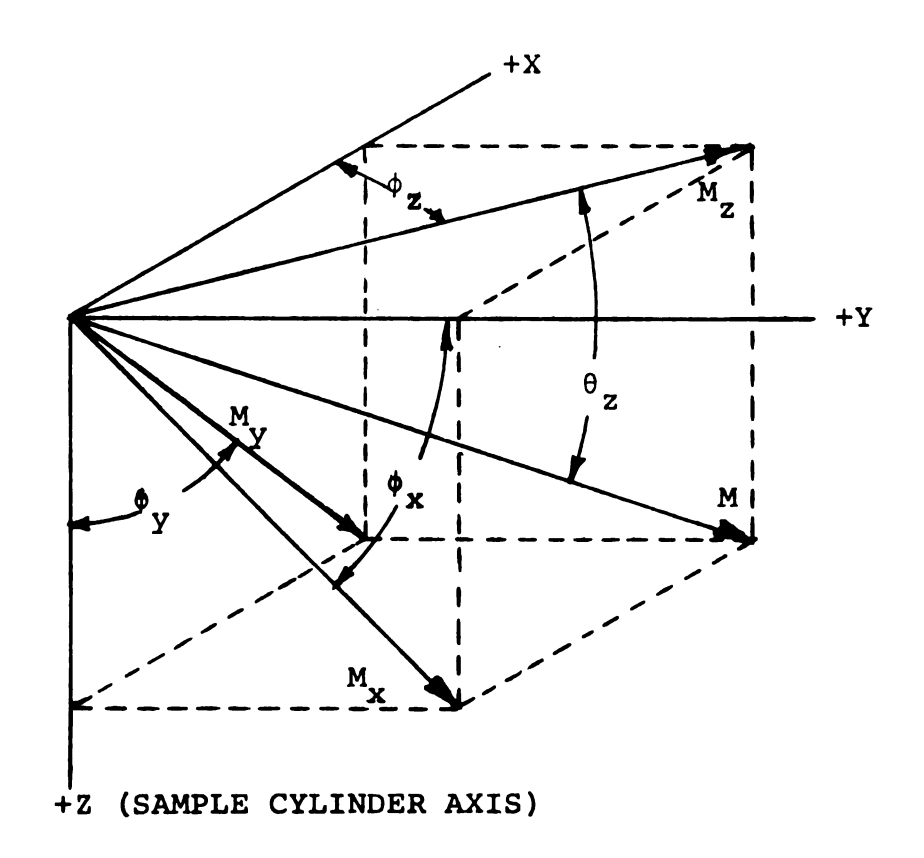


Figure 3. Identification of rock sample magnetic components.

instrument should measure the angle $\delta_{Z,a} = \delta_Z$, and $\delta_{Z,b} = 360^{\circ} - \delta_Z$ respectively for the two spins. The intensity of this component ideally should be equal for both spins, that is $M_{Z,a} = M_{Z,b} = M_Z$. The best values for δ_Z and M_Z are determined by averaging the data for the two spins. $\delta_Z = \frac{1}{2}(360^{\circ} + \delta_{Z,a} - \delta_{Z,b})$, and $M_Z = \frac{1}{2}(M_{Z,a} + M_{Z,b})$.

The other quantities 0_x , M_x , and 0_y and M_y are obtained in a similar manner by pairs of spins about the x and y axis. Relations between these measured angles and intensities are shown in Figure 3.

Figure 4 illustrates diagramatically how the signal is processed and measured. The rock sample is rotated at a constant speed in near proximity to a fixed pick up coil. The signal from the pick up coil is fed into the mixer and transferred directly to the high gain amplifier through the band pass filter to the oscilloscope for observation. The pick up coil signal also can be combined with the reference generator signal, amplified, filtered and observed on the oscilloscope.

The control console of the spinner magnetometer contains the brake clutch switch to turn "on" or "off" the mechanism of the magnetometer, the phase shifter, attenuator network, mixer circuit and a high gain amplifier.

The unknown pick up coil signal is compared with the reference generator signal of known phase and intensity.

Measurement of the pick up coil signal is made by simultaneously adjusting the phase and intensity of the reference

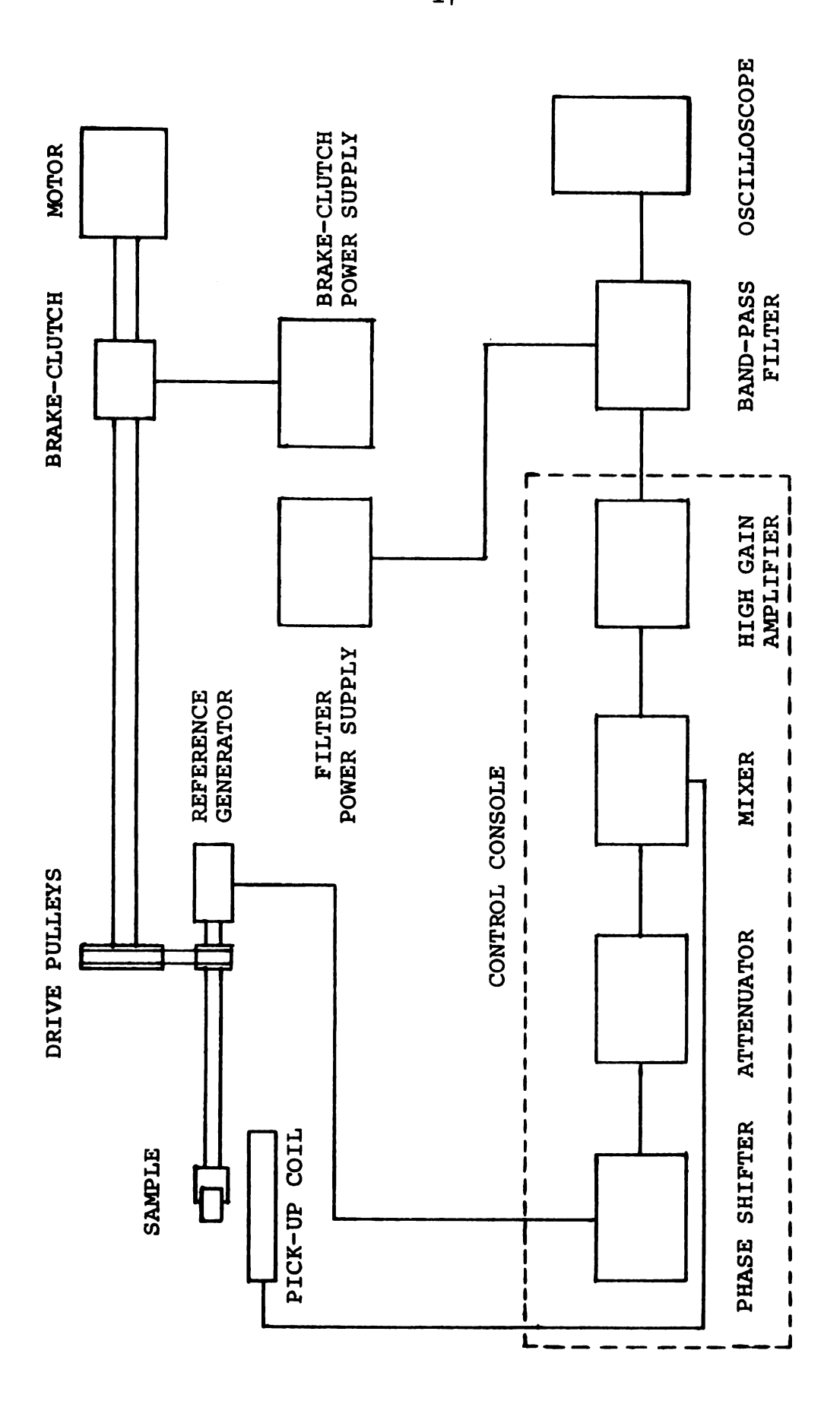
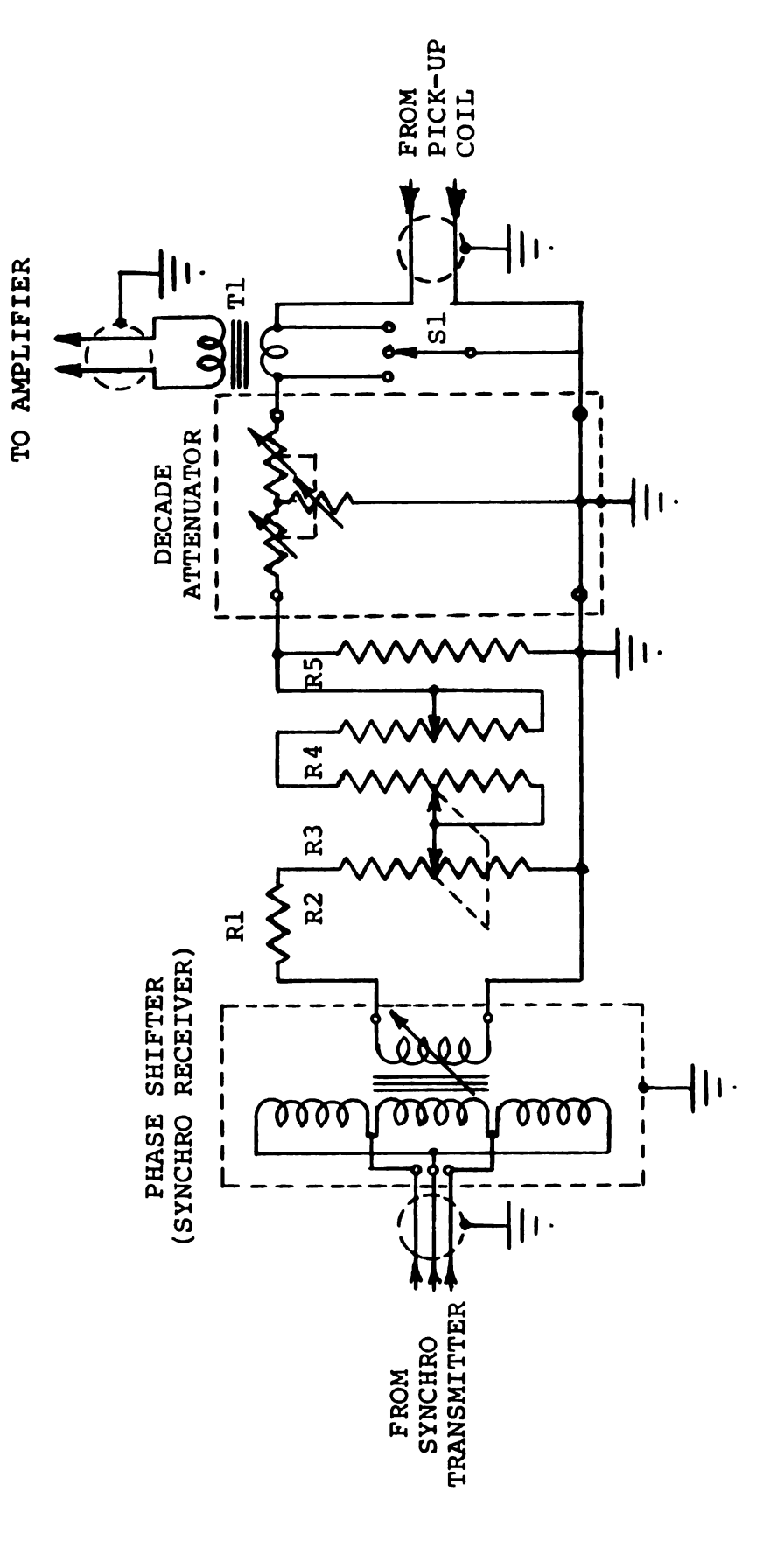


Figure 4. Block diagram of spinner magnetometer. (After MacClure, 1970)

signal to that of the pick up coil signal by turning the rotor of the synchro receiver (phase shifter) and adjusting the ten turn potentiometer (fine intensity) attenuator controls, until the oscilloscope indicates a null between the two signals.

The schematic diagram of the phase shifter, attenuator network, and mixer circuit is shown in Figure 5. The attenuator network consists of a fine intensity linear control, and a coarse intensity decade control. A three digit ten turn dial is used as the fine intensity control. The coarse intensity control is comprised of a single five step commercial T type voltage attenuator, that has a range of 0 to 100 db in 20 decibel steps. The attenuator network also contains a calibrating resistor which is used to calibrate the attenuator to read directly in emu between 1.00×10^{-5} to a three digit accuracy.

The mixer circuit consists of a single triple throw switch. The switch Sl in Figure 5 provides a means of observing the pick up coil signal, the reference generator signal, or these two signals combined. The normal mode of operation of the instrument is when these two signals are combined, and is obtained by placing the switch Sl in the neutral position. The secondary winding of the mixer transformer is connected to the input terminal of the high gain amplifier. The output of the amplifier is connected to the input of the band pass filter. The filter is adjusted to pass the operating frequency of the instrument



Schematic diagram of phase shifter, attenuator, and mixer circuits. (After MacClure, 1970) Figure 5.

which is 100 cps, and reject unwanted frequencies. This adjustment is made by four controls mounted on the band pass filter panels.

The output of the band pass filter is connected to the vertical input of the oscilloscope, which is used to observe the output signal of the instrument.

The sample whose direction and intensity of NRM are to be measured is inserted into a cubical sample holder and properly aligned. The sample holder is then inserted into the magnetometer head, and the measurements and recordings are made according to the operational procedure for the spinner magnetometer outlined by MacClure (1970).

A source of error is the misalignment of the rock sample in the cubical sample holder. Doell and Cox (1965) investigated the effects of correlation of axes of rock samples and cubical holder when the sample was removed from the holder between measurements. They determined the discrepancies to be 0.7 percent for the direction, and 1.1 percent for the intensity of a sample.

The internal consistency of the spinner magnetometer was determined using a magnetically stable rock sample by MacClure (1970). Fifteen measurements were taken by him over a period of four days, without removing the sample from the sample holder between successive measurements. The percentage of error of the standard deviation to the mean in relative form for the intensity was 1.87 percent for the † z axes, and 0.24 percent for the phase angle.

CHAPTER V

MEASURED MAGNETIC ROCK PROPERTIES

The samples used in this study are from 33 sites from the northern portion of the Boulder Batholith. Fifteen of these sites are in the marginal Unionville granodiorite, and 18 of the sites are from the interior Clancy granodiorite. The traverse of these sites is shown in Figure 1, which is a generalized geologic map of the area and the locations of sample sites with respect to the analyzed magnetic profile are shown in Figure 27b.

After the initial measurements of NRM were made, the samples from all the sites were a.f. demagnetized to eliminate secondary components of magnetization which may have been acquired while drilling the sample and cutting it to size and during storage for about two years in the laboratory. The a.f. demagnetization apparatus used is similar in design to the apparatus described by Doell and Cox (1967). In this apparatus a sample is tumbled within an alternating magnetic field so as to constantly change the orientation of the specimen within the magnetic field, meanwhile the peak strength of the field is slowly reduced to zero. The a.f. demagnetization apparatus accomodates the cubical sample holders used in the spinner magnetometer, and all

measurements and a.f. demagnetization on a sample can be made without removing the sample from its holder.

Samples from 17 sites from both the rock types in the area were a.f. demagnetized at levels of 50, 125, 250 and 400 oersteds. These levels of a.f. demagnetization were selected on the basis of some preliminary trials on a few samples at 17 levels from 25 to 800 oersteds. After reviewing the results obtained by demagnetizing samples from these sites, it was found that dispersion of the directions of NRM for many sites was a minimum after demagnetizing at a level of 125 oersteds. The samples from the remaining 16 sites were therefore demagnetized at only this level.

The mean direction of NRM of all the samples in a site, the circle of confidence <>95, and the precision parameter K were obtained using methods described by Fisher (1953). A computer program written by D. D. Sanderson was used for the calculation of these parameters. The circle of confidence <>95 is a circle whose radius includes 95 percent of the individual directions of NRM of samples within a group or site. These circles are centered on the true mean. The smaller the radius, the lower is the scatter in the directions of NRM. The precision parameter K determines the dispersion of magnetic directions of individual samples within a group or site, the larger its value, the closer the directions converge on the true mean. Results from samples which deviate markedly from the results of the rest of the samples from a site were excluded from the final

results and thus were not used in the calculations of these parameters. Cores from some sites had more than one sample per core. After the initial measurement of NRM was made on these samples, an average direction and intensity of NRM was obtained, and then the samples were treated as one sample in the calculation of site averages. In general, it was found that within core dispersion was very much less than between core dispersion.

Sites which had a circle of confidence ≪95 larger than 30° were arbitrarily excluded from calculating the average NRM of a rock type. Nineteen of the 33 sites had a circle of confidence of 30° or less. Eight of these sites are from the Unionville granodiorite, and ll sites are from the Clancy granodiorite. The directions and intensity of NRM (both before and after demagnetization), the average susceptibility of samples from a site, the Q factor (ratio of NRM to induced magnetism) and Fisher's parameters for the sites from the Unionville granodiorite are shown in Table II. The same parameters of the Clancy granodiorite are shown in Table III. The total intensity of the earth's field in the area was estimated to be 59,000 %. The directions of NRM for sites with a circle of confidence less than 30° are presented in Figures 6A through Figures 24B. The direction of the earth's magnetic field in the area is represented by "x" in these figures. The NRM vectors above the horizon are indicated by "o", and those below are indicated by ".",

Table II: Magnetic Properties of the Unionville Granodiorite

Site	drings Samples Pemagnetizing In Cersteds	Mean Dec. In Degrees	Mean Inc. In Degrees	Radius of Confidence (295) in Deg.	Precision Parameter K	Int. of NRM X10-6 emu/cc.	Sus.X10-6 emu/cc.	Q Factor	Density in gm/cc.
UN 1	7 50 125 250 400	329.5 339.6 348.0 357.4 339.1	43.9 52.2 62.6 70.0 70.4	28.2 23.8 16.0 26.1 23.6	5.6 7.4 15.2 6.3 7.5	343.9 229.7 138.8 135.2 93.5	2510	0.23 0.16 0.09 0.09 0.06	2.68
UN 2	5 50 125 250 400	84.3 138.8 143.8 138.7 136.2	86.0 84.0 81.6 80.6 80.7	50.5 49.3 49.1 48.4 47.4	3.4 3.4 3.5 2.6	1292 829.6 805.2 626.4 467.4	2960	0.74 0.49 0.46 0.36 0.27	2.75
UN 3	8 125	45.6 56.2	65.8 70.4	4.0 3.6	1930 244.7	1104.1	3190	0.55 0.37	2.72
UN 4	7 125	21.4 57.4	49.5 49.1	21.1 36.7	9.2 3.7	929.7 424.0	3640	0.43	2.77
UN 5	8 125	38.1 46.6	75.3 73.0	9.1 8.6	38.1 42.8	2082.5	3130	1.13 0.83	2.72
un 6	50 125 250 400	321.1 343.6 351.5 325.8 351.1	45.2 51.7 60.5 63.4 62.0	30.9 32.3 35.6 43.2 42.0	7.1 6.6 5.6 5.5 4.3	377.2 231.6 152.0 88.8 79.78	3290	0.19 0.12 0.08 0.05 0.04	2.68
UN 7	5 125	72.0 68.9	45.9 37.7		7.8 3.5	639 461	3100	0.35 0.25	2.69
UN 8	50 125 250 400	131.9	52.4 -6.6 -3.8 -10.7 -15.4	142.2	1.5 1.5 2.0 1.8 1.9	310.9 389.3	3430	0.13 0.15 0.19 0.07 0.05	2.69
HC 1	8 50 125 250 400	2.7	74.1 69.4 73.1 56.7 74.5	36.5 23.4 31.5 40.0 52.0	2.9	392.6 276.0 131.9 51.7 34.3	2020	0.33 0.23 0.11 0.04 0.03	2.7

Site	Samples Demagnetizing In Oersteds	Mean Dec. In Degrees	Mean Inc. In Degrees	Radius of Confidence (~95) in Deg.	Precision Parameter K	Int. of NRM X10-6 emu/cc.	Sus.X10-6 emu/cc.	Q Factor	Density in gm/cc.
HC 2	6 125	126.1 213.2	89.2 81.3	44.4 29.9	3.9 6.0	620 173	3100	0.34 0.09	2.66
HC 3	6 125	5.7 19.7	67.0 71.3	37.0 22.4	4.2 9.9	1529 528.8	2400	1.08	2.68
HC 4	7 125		66.4 69.6	91.9 68.7		1925 876.4	1690	1.93 0.88	2.69
HC 5	5 125		59.2 75.9	60.4 52.0	2.6 3.1	5206 2854	980	9.0 4.9	2.8
нс 6	7 50 125 250 400	45.5 48.3 49.7 47.9 46.7	73.8 71.9 74.3 72.3 71.7	7.67 7.01 10.04 7.21 7.02	77.3 92.4 45.5 87.4 92.1	4440 32 45 311 7 2975 2753	2720	2.77 2.02 1.94 1.85 1.72	2.74
HC10	7 50 125 250 400	38.0 36.5 27.5 24.7 24.2	58.6 62.3 68.9 70.0 70.2	30.5 26.5 21.4 21.1 21.1	6.1 8.9 9.1	4405.7 4315.7 3985.7 3558.5 3055.5	2860	2.61 2.56 2.36 2.11 1.81	2.76

Table III: Magnetic Properties of the Clancy Granodiorite

Site	Number Samples Demagnetizing In Oersteds	Mean Dec. In Degrees	Mean Inc. In Degrees	Radius of Confidence (~95) in Deg.	Precision Parameter K	Int. of NEM X10-6 emu/cc.	Sus.X10-6 emu/cc.	Q Factor	Density in gm/cc.
CL 1	6 50 125 250 400	276.2 256.9 241.5 240.0 230.5	-58.6	18.5	4.6 6.1 16.5 14.0	66.9 72.1	3110	0.05 0.04 0.04 0.03 0.02	2.58
CL 2	8 50 125 250 400	265.4 231.7 218.5 211.4 214.1	-81.0 -80.1 -79.9	9.0 6.6 7.4	10.1 39.1 70.5 57.7 20.0	464 410 419 355 219	2020	0.39 0.34 0.35 0.30 0.18	2.61
CL 3	7 125	322.4 282.8	40.1 5.2	29.1 22.3	5.3 8.3	244 142	2640	0.16 0.09	2.55
CL 4	8 12 5	285.7 191.1	-9.8 -47.9		1.4	139 98	2970	0.08 0.06	2.62
CL 5	7 125	347.4 353.4	69.8 71. 1	13.6 19.3	20.6	307 132	2940	0.18 0.08	2.53
CL 6	6 125	268.9 288.6	73.0 73.9	91.6 57.8		1119 509	3170	0.6	2.6
CL 7	5 50 125 250 400	321.5 320.9 247.0 258.3 203.1	73.4 80.2 82.2 78.1 79.8	16.7 27.2 38.5	8.9 4.9	330.0 169.6 101.8 80.2 71.2	3310	0.17 0.09 0.05 0.04 0.04	2.58
CL 8	7 50 125 250 400	356.6 357.8 359.4 2.6 3.5	63.2 65.2 66.0 65.8 65.6	12.5 12.3 12.4	24.2 25.1 24.6	823.9 687.6 612.9 514.3 395.4	2530	0.55 0.46 0.41 0.39 0.26	2.65
CL 9	6 125	274.1 333.4		108.5 97.1		103.3 46.9	2650	0.66 0.30	2.49
CL10	5 125	38.4 24.7	57·9 59·6			723 4 7 8	2560	0.48	2.55

Site	Number	Demagnetizing Telagenetizing In Oersteds	Mean Dec. In Degrees	Mean Inc. In Degrees	Radius of Gircle of Confidence Confidence	Precision Parameter K	Int. of NRM X10-6 emu/cc.	Sus.X10-6 emu/cc.	Q Factor	Density in gm/cc.
CL11	7	50 125 250 400	17.0 21.5 23.6 24.5 25.9	65.1 65.3 64.4 64.6 65.6	7.3 7.8 8.1 9.0	69.3 60.6 56.1	1085 910 885 783 631	2440	0.75 0.63 0.61 0.54 0.44	2.61
CL12	8	125	15.0 16.6	59.0 69.1	22.4 53.8		511.4 217	303	0.29 0.12	2.69
CL13	8	50 125 250 400	65.2 46.2 42.2 41.3 39.6	67.6 64.5 64.3 63.9		141.1 164.8	1465 1142 1069 956 918	2580	0.96 0.75 0.7 0.63 0.60	2.62
CL14	6	50 125 250 400	328.0 329.2 334.9 337.2 2.3	46.9 52.3 57.8 59.9 55.6	27.0 26.5 26.4 24.5 20.7	7.4 8.4	259.8 223.5 129.1 74.2 46.9	1020	0.43 0.37 0.21 0.12 0.08	2.47
CL15	8	50 125 250 400	333.0 195.6 313.7	15.2 3.6 -10.5 28.1 66.5	145.3 78.3 106.7 111.0 105.5	1.1 1.3 1.2 1.3	1923.7	1160	3.38 2.81 1.01 0.68 0.37	2.53
CL16	8	125	353.3 356.0	51.1 49.0	14.3 15.7	15.9 13.4	134 88	412	0.55 0.36	2.57
HC 7	5	125	46.9 33.3	-2.3 20.6	61.9 51.3	2.5 3.2	2610 107 7. 2	3400	1.3 0.54	2.64
HC 8	6	125	54.2 122.5	71.7 79.0	40.9 31.7	3.6 4.6	150 135	3250	0.08 0.07	2.66

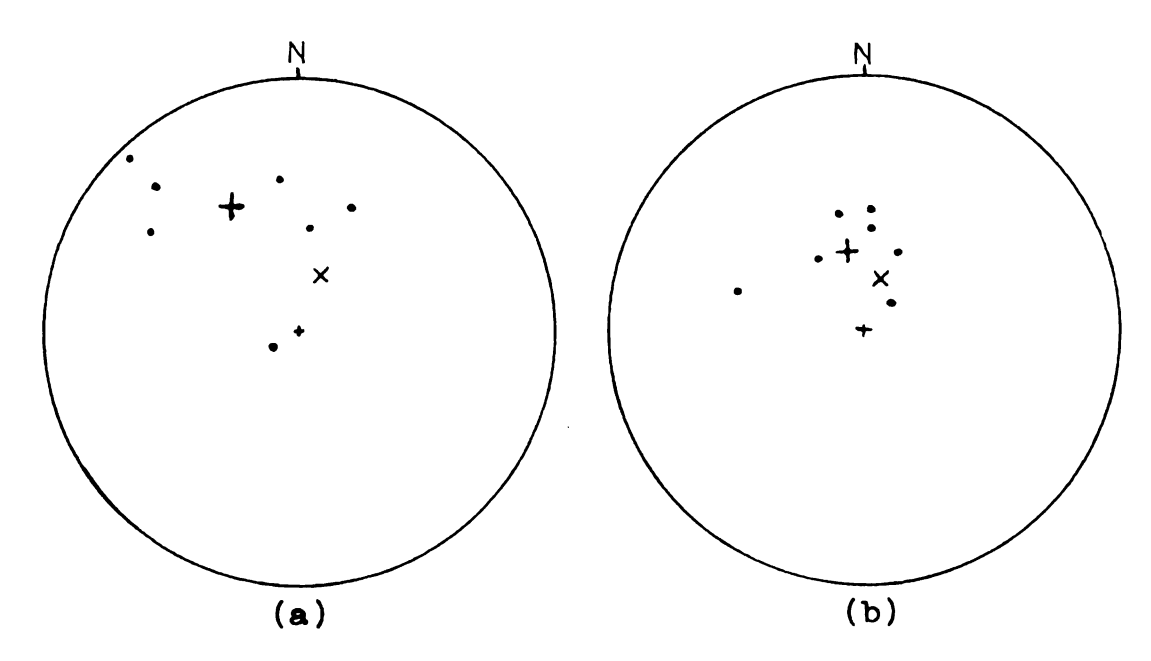


Figure 6. Equal area projection for samples from site UN-1
(a) before a.f. demagnetization
(b) after a.f. demagnetization at 125 oersteds

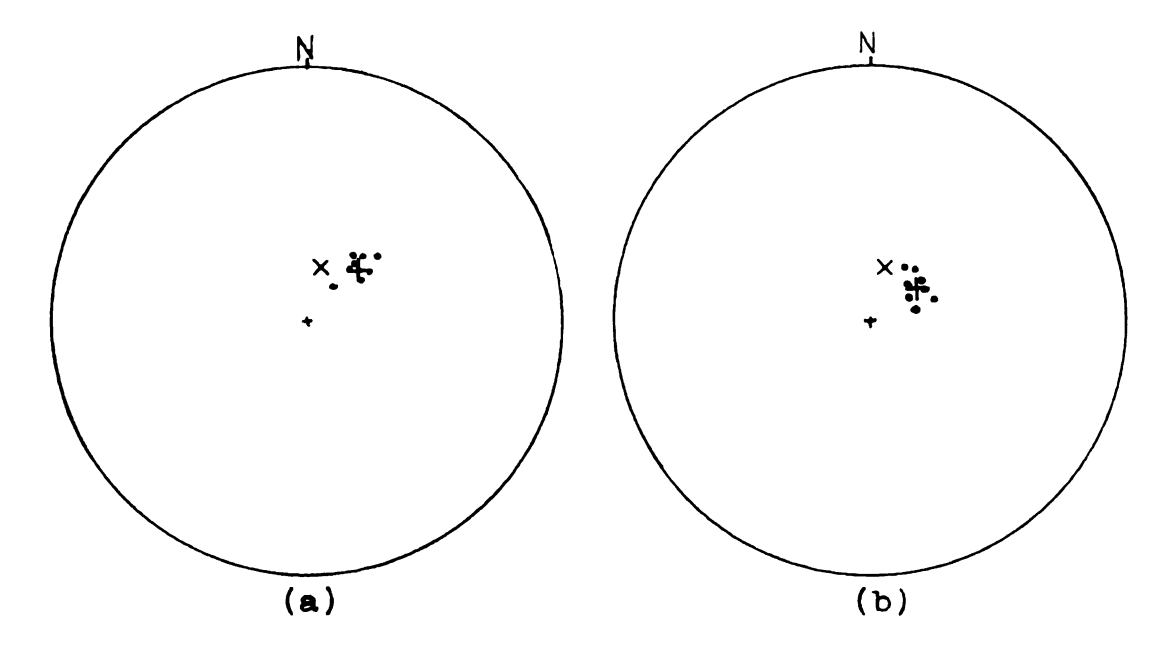


Figure 7. Equal area projection for samples from site UN-3 (a) before a.f. demagnetization (b) after a.f. demagnetization at 125 oersteds

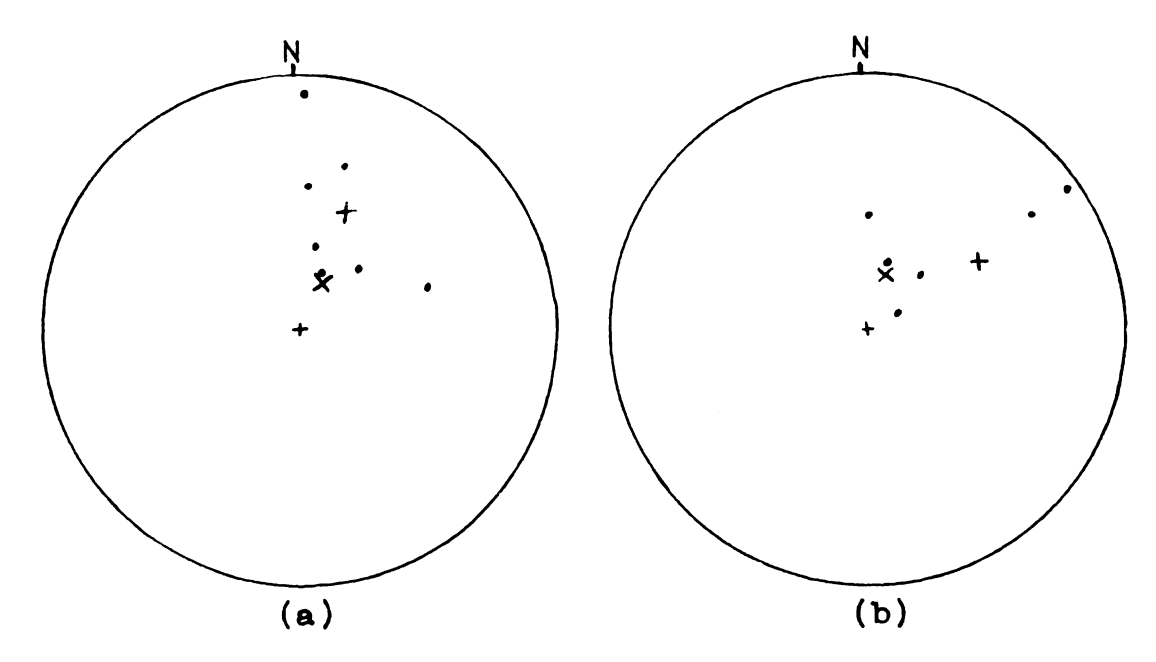


Figure 8. Equal area projection for samples from site UN-4 (a) before a.f. demagnetization (b) after a.f. demagnetization at 125 oersteds

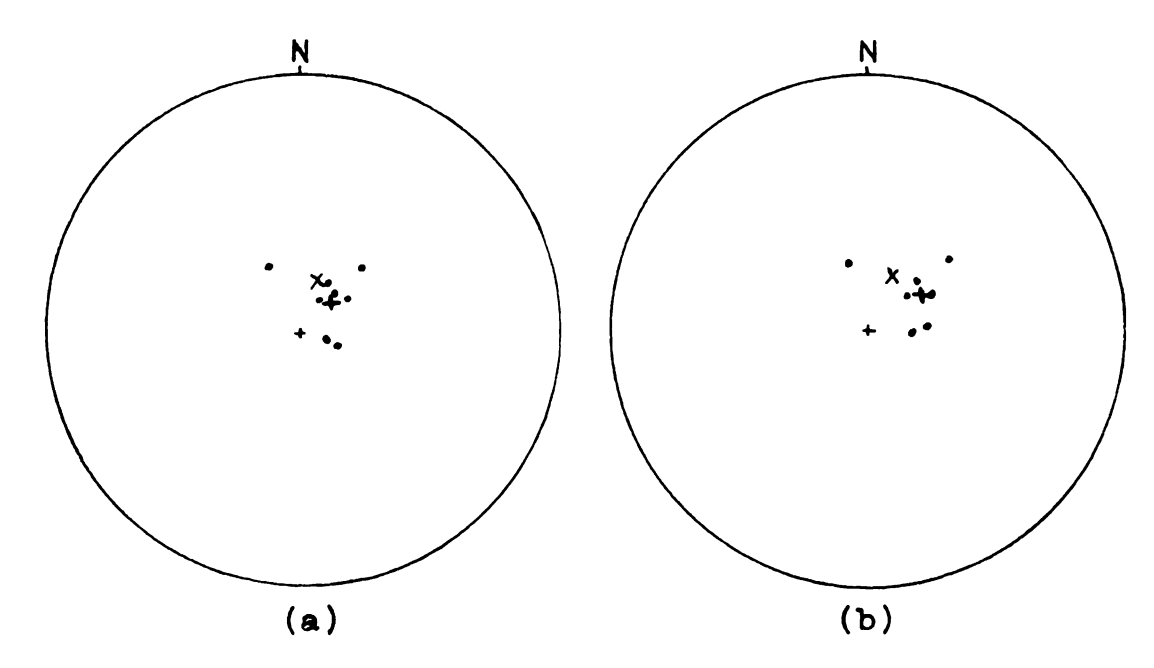


Figure 9. Equal area projection for samples from site UN-5 (a) before a.f. demagnetization (b) after a.f. demagnetization at 125 oersteds

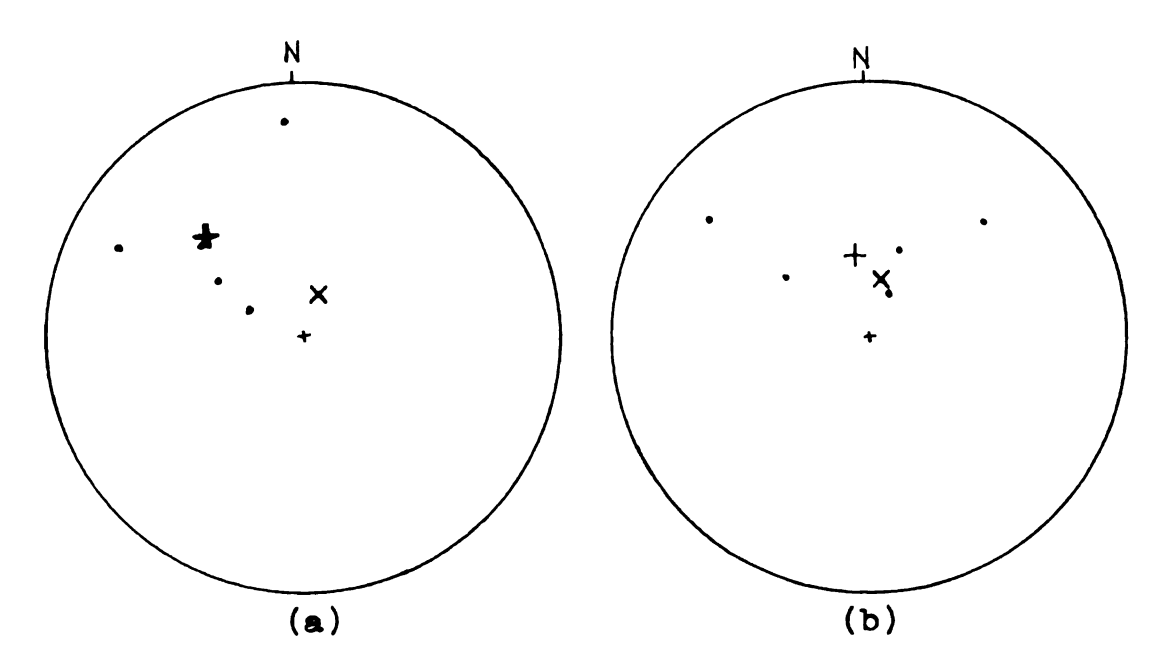


Figure 10. Equal area projection for samples from site UN-6 (a) before a.f. demagnetization (b) after a.f. demagnetization at 125 oersteds

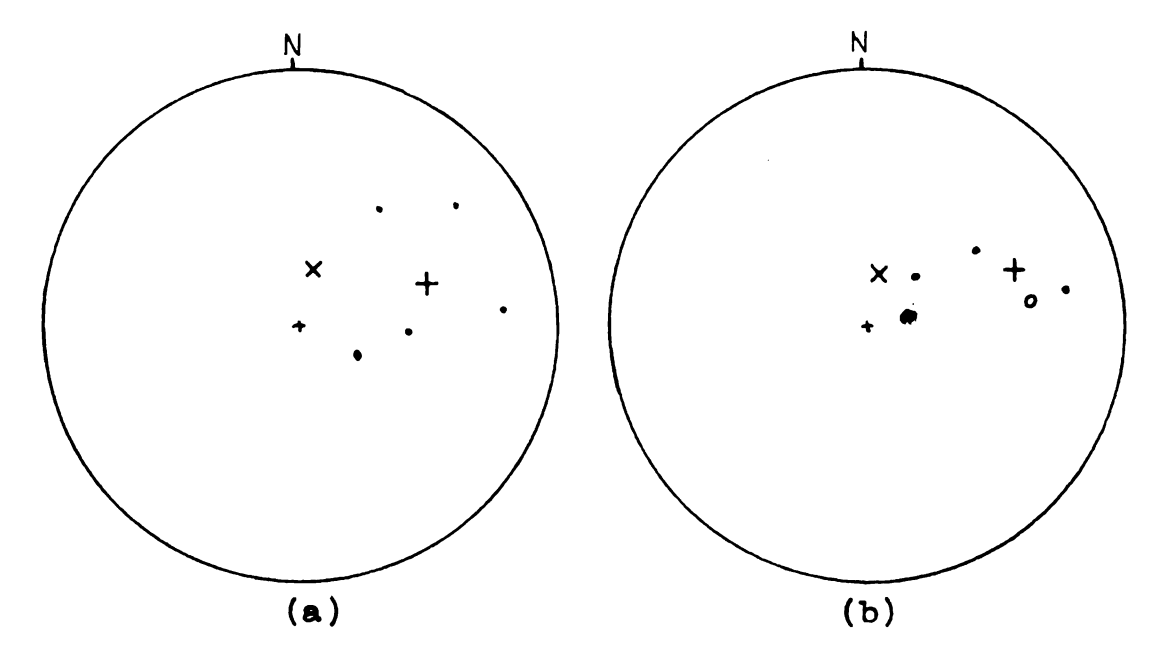


Figure 11. Equal area projection for samples from site UN-7 (a) before a.f. demagnetization (b) after a.f. demagnetization at 125 oersteds

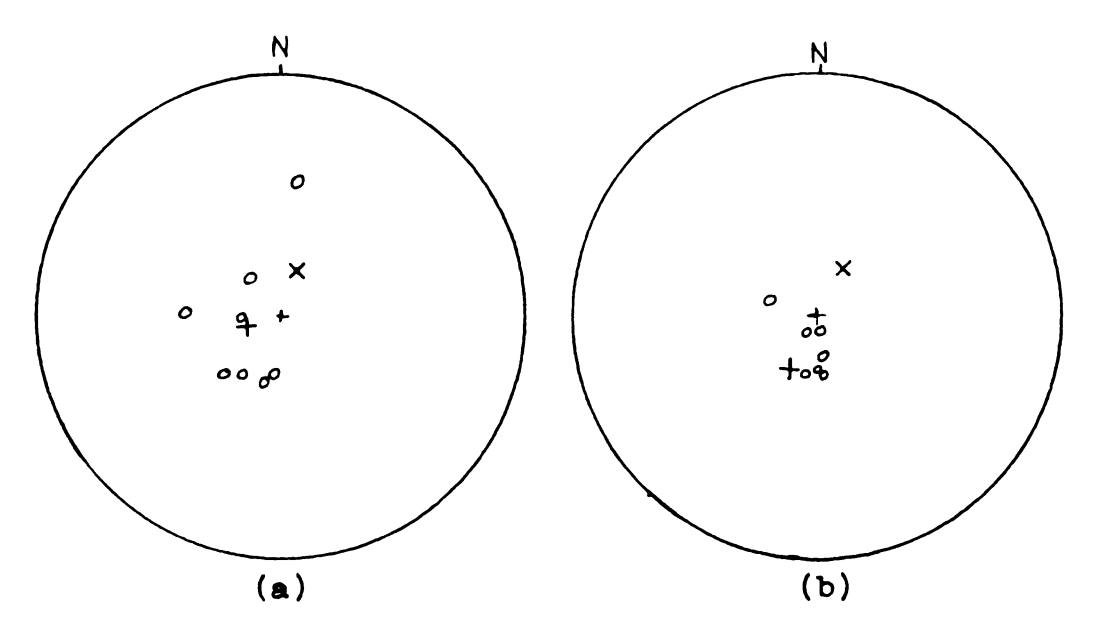


Figure 12. Equal area projection for samples from site CL-2 (a) before a.f. demagnetization (b) after a.f. demagnetization at 125 oersteds

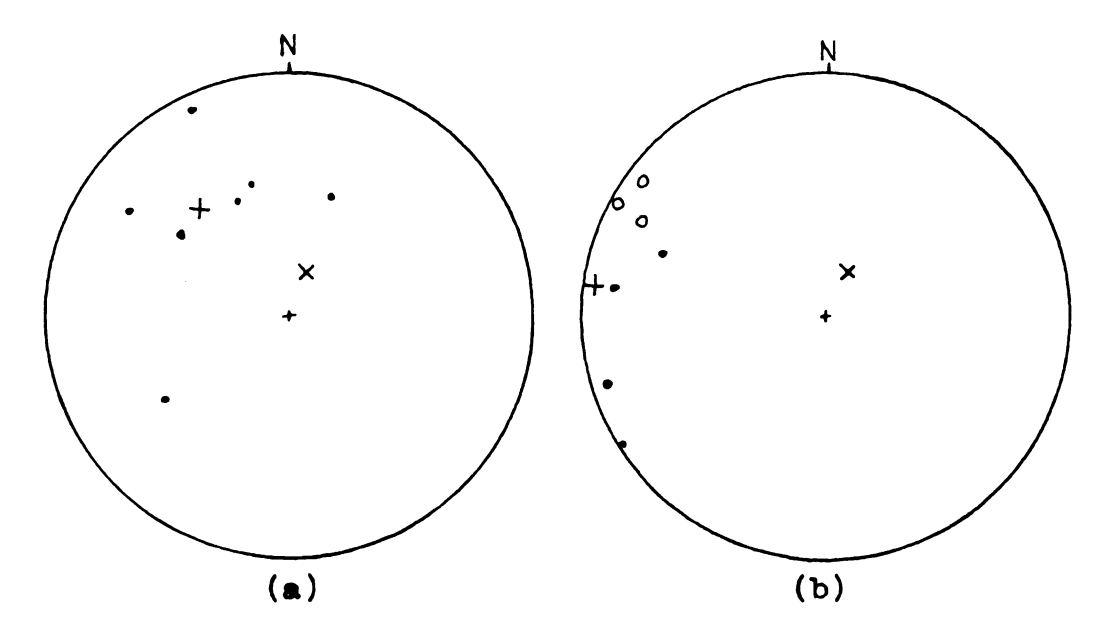


Figure 13. Equal area projection for samples from site CL-3 (a) before a.f. demagnetization (b) after a.f. demagnetization at 125 oersteds

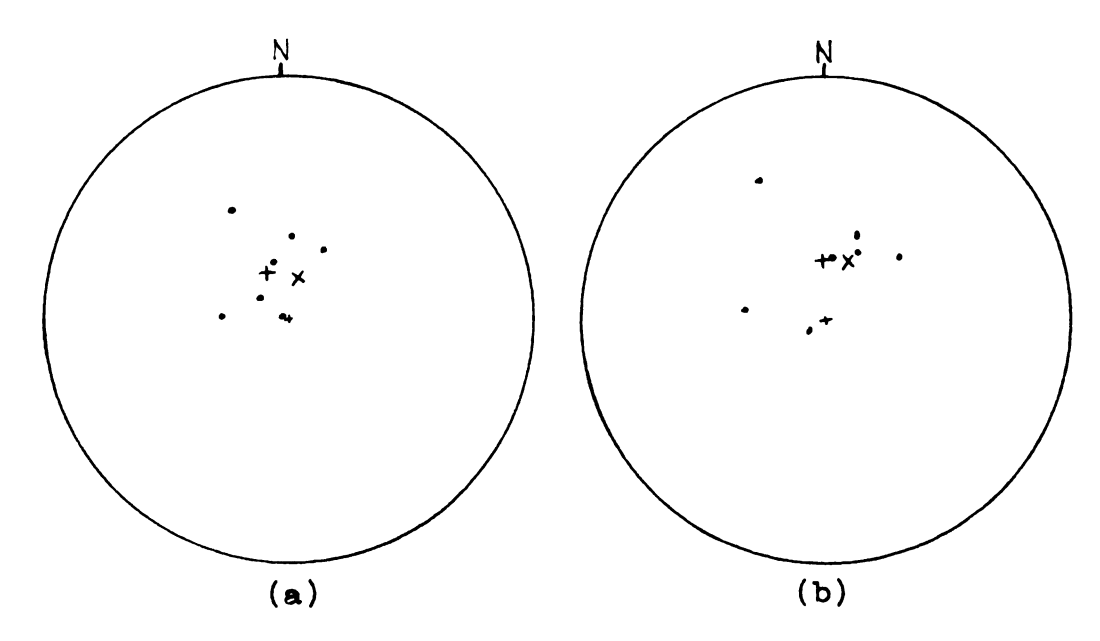


Figure 14. Equal area projection for samples from site CL-5 (a) before a.f. demagnetization (b) after a.f. demagnetization at 125 oersteds

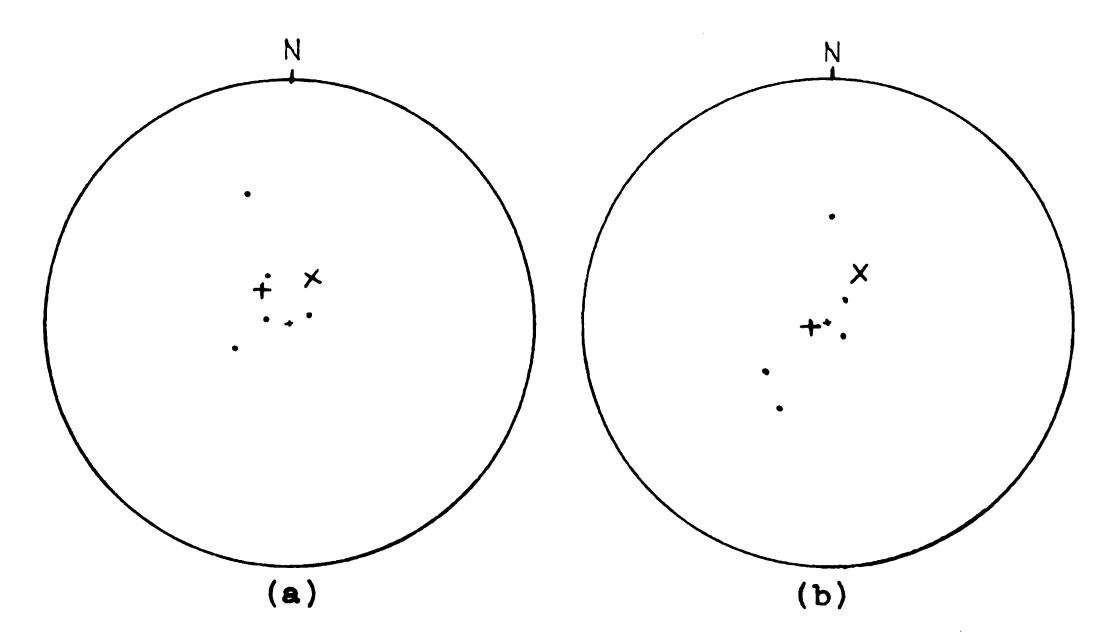


Figure 15. Equal area projection for samples from site CL-7
(a) before a.f. demagnetization
(b) after a.f. demagnetization at 125 oersteds

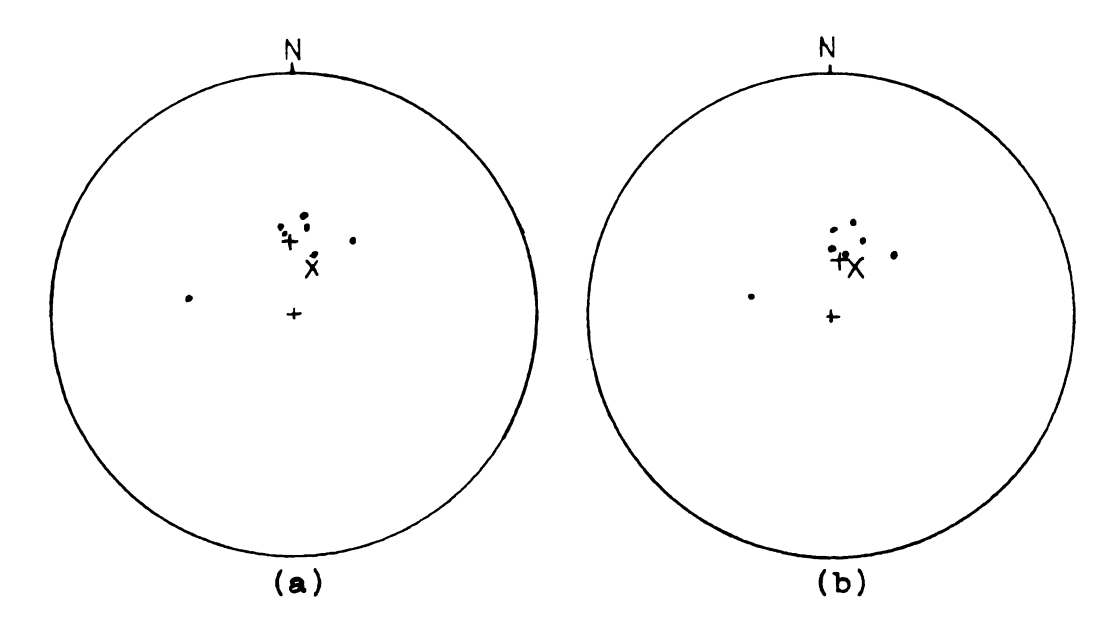


Figure 16. Equal area projection for samples from site CL-8 (a) before a.f. demagnetization (b) after a.f. demagnetization at 125 oersteds

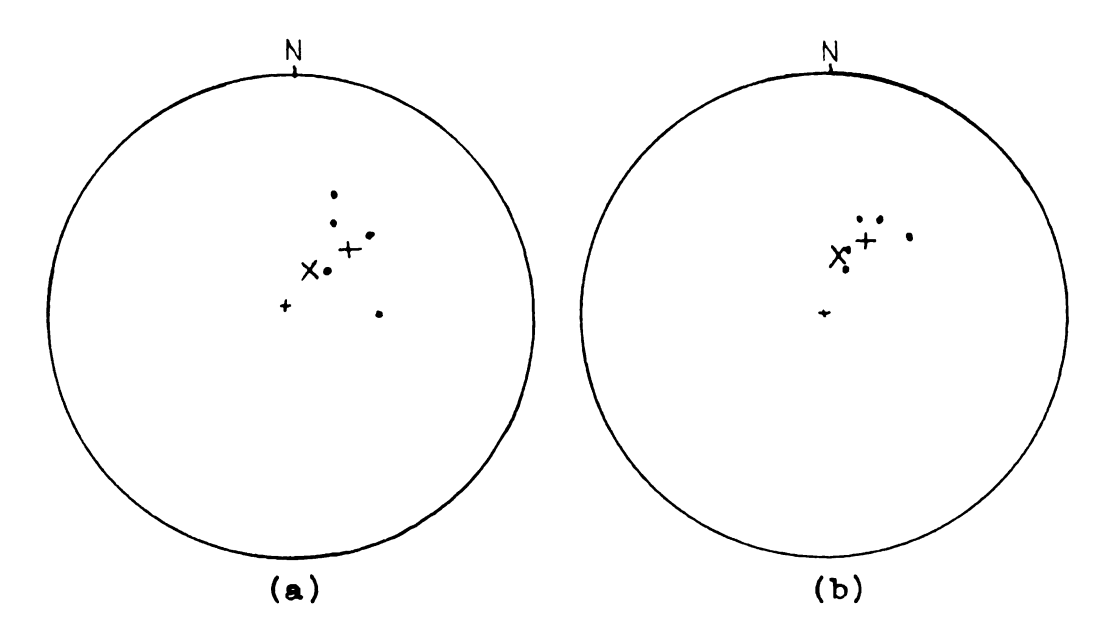


Figure 17. Equal area projection for samples from site CL-10 (a) before a.f. demagnetization (b) after a.f. demagnetization at 125 oersteds

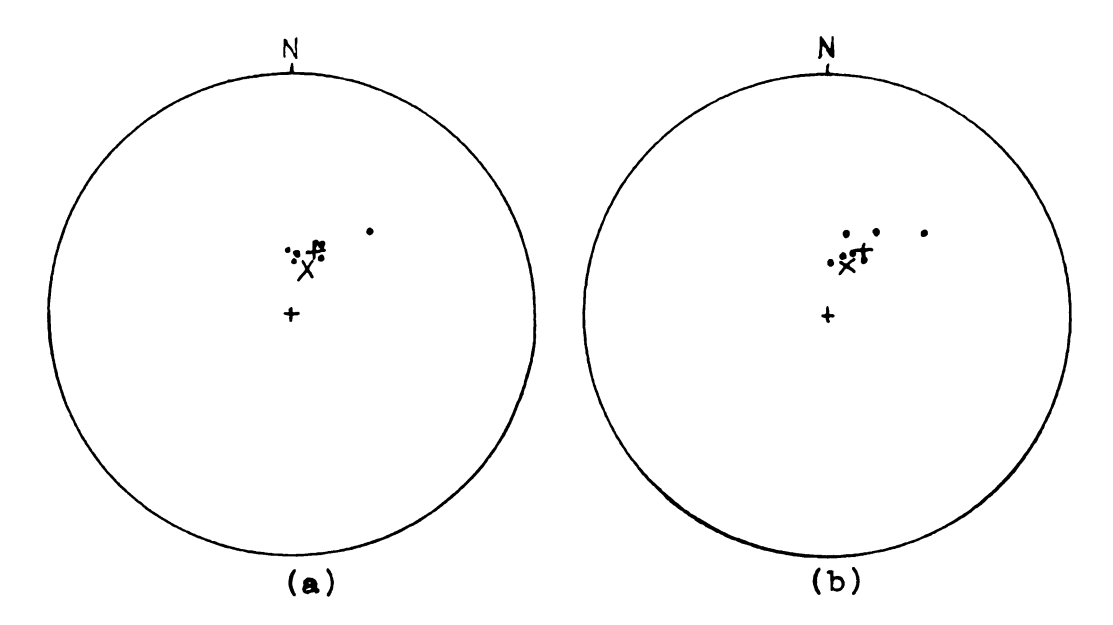


Figure 18. Equal area projection for samples from site CL-11 (a) before a.f. demagnetization (b) after a.f. demagnetization at 125 oersteds

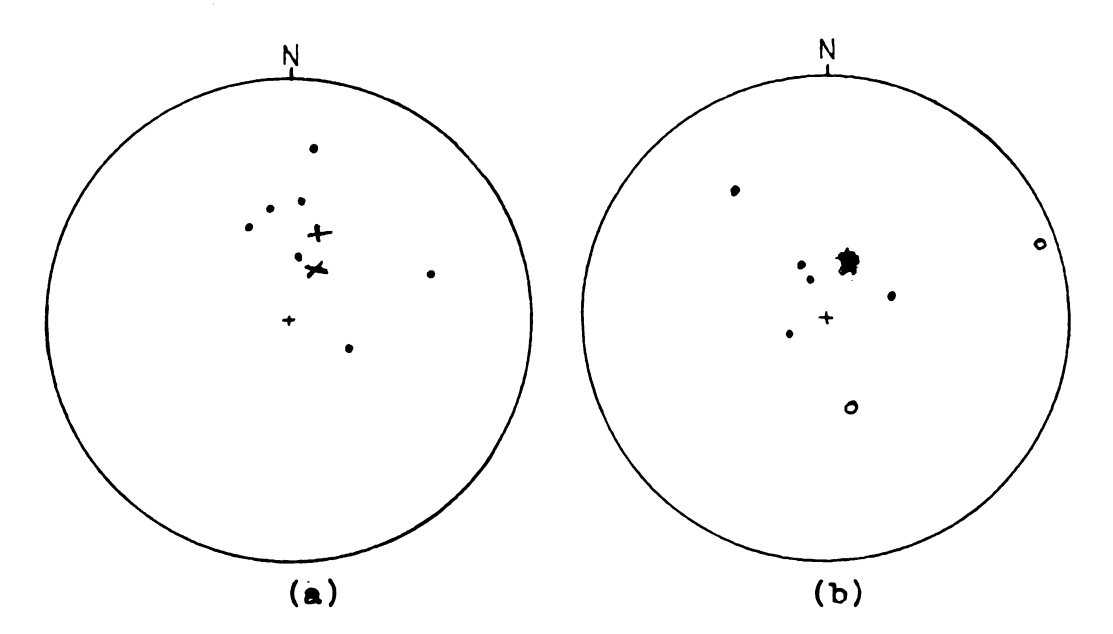


Figure 19. Equal area projection for samples from site CL-12 (a) before a.f. demagnetization (b) after a.f. demagnetization at 125 oersteds

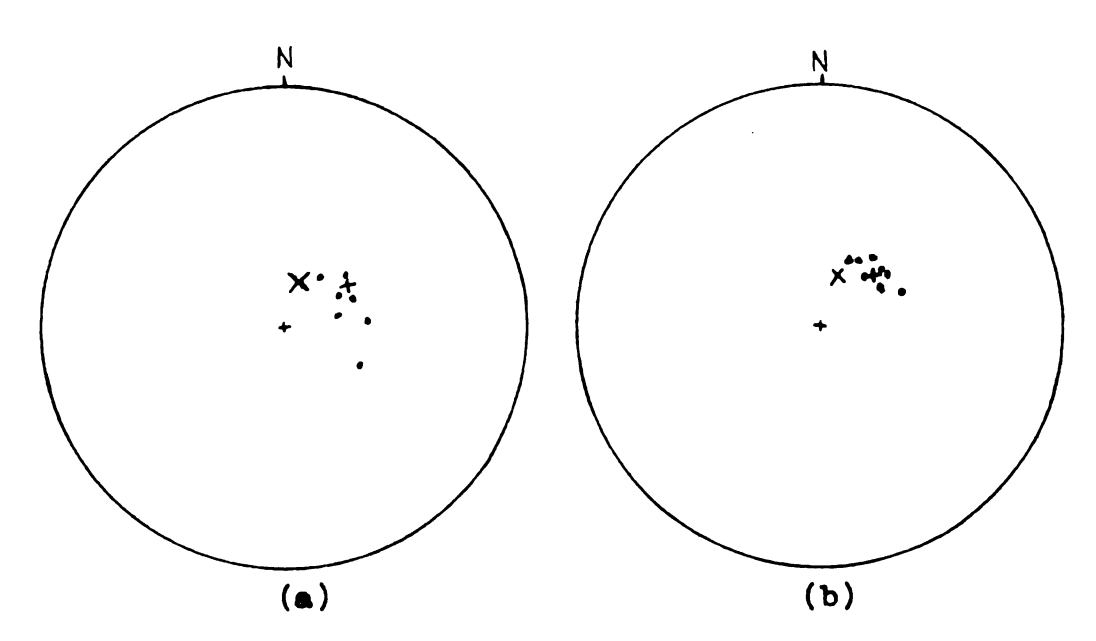


Figure 20. Equal area projection for samples from site CL-13 (a) before a.f. demagnetization (b) after a.f. demagnetization at 125 oersteds

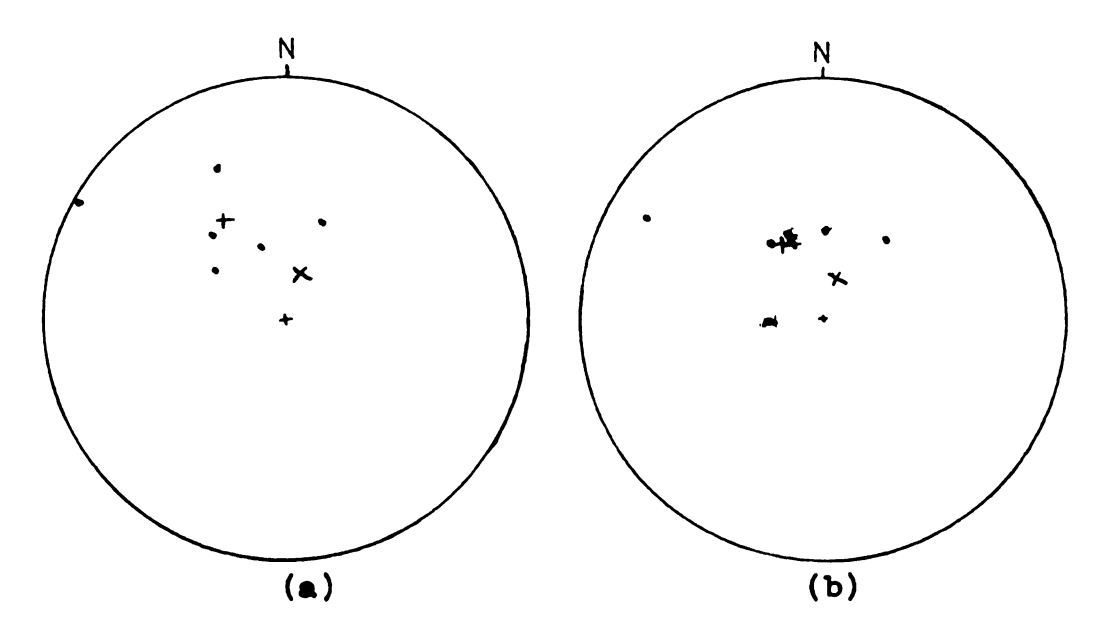


Figure 21. Equal area projection for samples from site CL-14
(a) before a.f. demagnetization
(b) after a.f. demagnetization at 125 oersteds

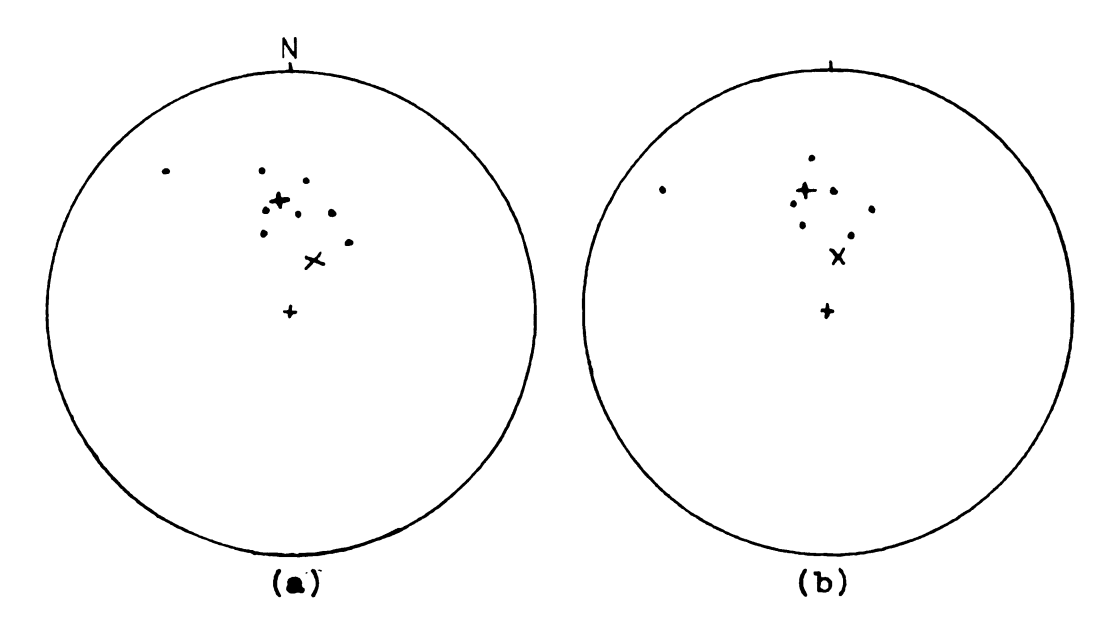


Figure 22. Equal area projection for samples from site CL-16 (a) before a.f. demagnetization (b) after a.f. demagnetization at 125 cersteds

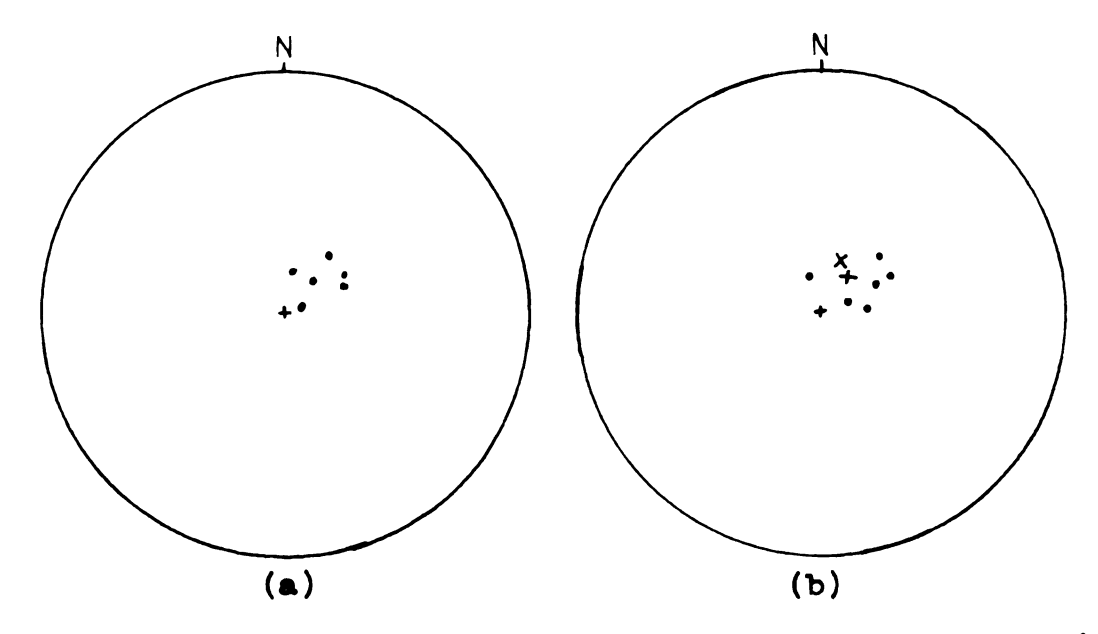


Figure 23. Equal area projection for samples from site HC-6 (a) before a.f. demagnetization (b) after a.f. demagnetization at 125 oersteds

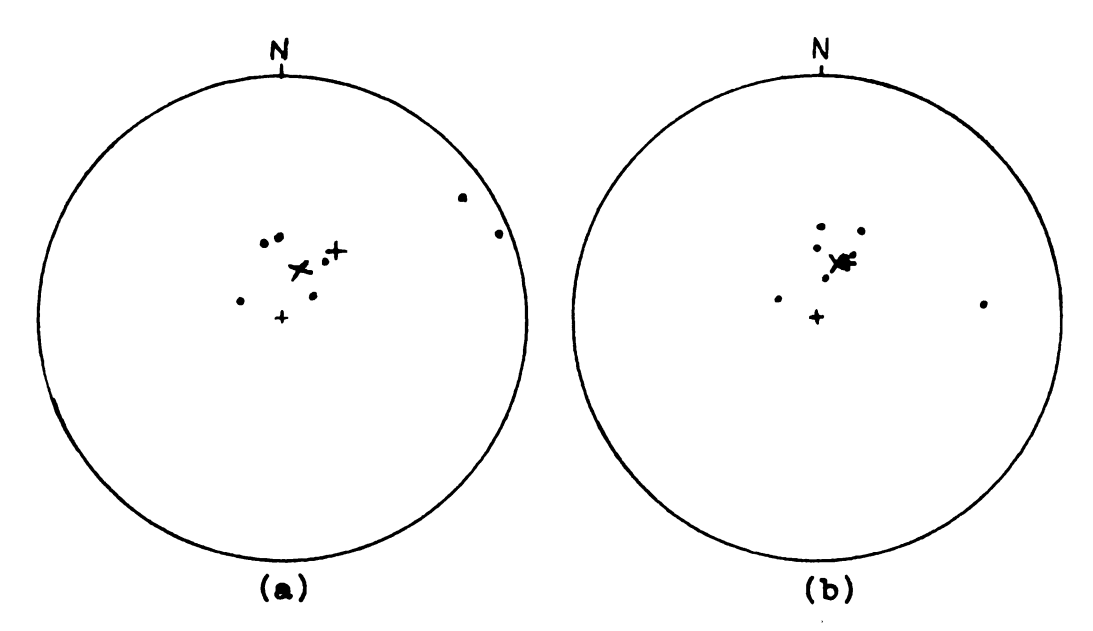


Figure 24. Equal area projection for samples from site HC-10 (a) before a.f. demagnetization (b) after a.f. demagnetization at 125 oersteds

and the mean direction of NRM within a site is represented by $^{n+n}$ in these figures.

The susceptibility of 237 samples from the 33 sites range from 410 to 3640x10⁻⁶ emu per cc, with an average of 2730x10⁻⁶ emu per cc for sites in the Unionville granodiorite, and an average of 2510x10⁻⁶ emu per cc for sites in the Clancy granodiorite. There was no significant difference in susceptibilities between the two rock types. However, when the average susceptibility of the sites is plotted against the distance of the sites from the contact of the batholith with the surrounding sediments, as shown in Figure 25, a linear correlation is found between the average susceptibility of a site in the Clancy granodiorite and the distance of the site from the contact. The correlation coefficient is -0.63, which indicates that the susceptibility of these sites decreases with respect to distance from the intrusive contact. No relationship was found between the intensity of NRM, inclination and declination of NRM. and precision parameters for either the Unionville or the Clancy granodiorite with respect to distance of a site from the contact.

The decrease in susceptibility for the samples from the Clancy granodiorite with respect to distance from the contact is probably due to a decrease in the volume percent of magnetite. This could result from a primary difference in magnetite content due to magnetic differentiation within the cooling batholith or from subsequent alteration of

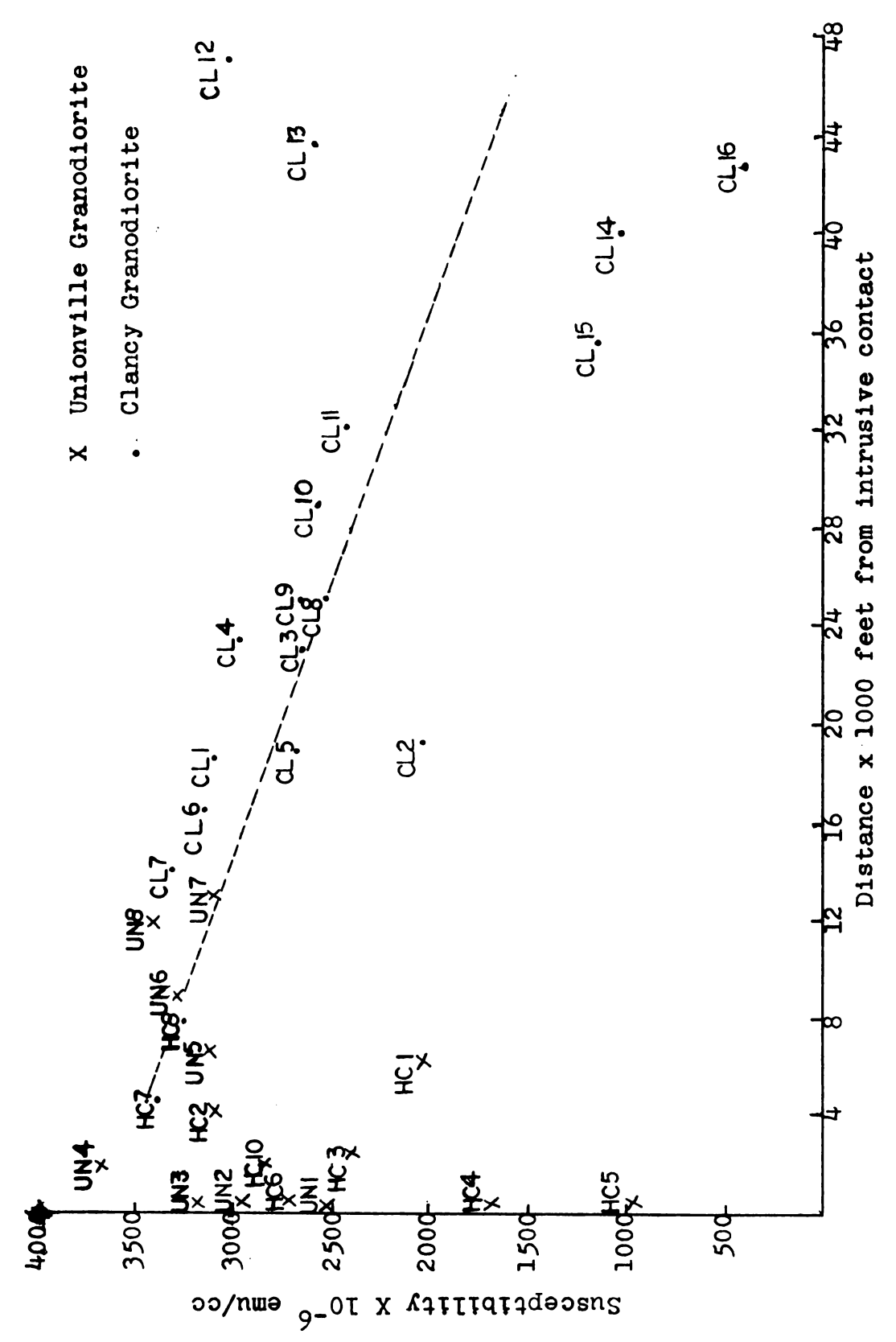


Figure 25. Relationship between magnetic susceptibility of Clancy grano-diorite and distance from intrusive contact

magnetite to non-magnetic minerals on a batholith wide basis. Hanna (1969) has noted magnetic minimums associated with portions of the Boulder Batholith that have been highly altered. The altered rocks have negligible magnetic properties. However, these alteration zones are local phenomena compared to the scale of the relationship discussed here. Furthermore, only fresh unaltered samples were collected for the magnetic property study. Therefore, it is suggested that the origin of the observed relationship between the magnetic susceptibility of the Clancy granodiorite and the distance from the Boulder Batholith contact is in the primary variation of the magnetite content. However, the origin and validity of this relationship cannot be resolved without further sampling in other areas of the batholith and detailed petrology, i.e., analysis of the magnetite content, the degree and the type of alteration, and the composition and magnetic susceptibility of the magnetic minerals.

A tentative conclusion suggested by the fact that magnetic susceptibility of the Unionville granodiorite does not fit into the magnetic susceptibility versus distance to the contact of the Clancy granodiorite relationship is that the Unionville and Clancy granodiorite represent separate magmatic phases. This conclusion substantiates Klepper's (1962) statement that the Unionville is older than the Clancy granodiorite.

After the samples from all sites were a.f. demagnetized it was observed that in general the dispersion of directions of NRM of samples within a site decreased with a.f. demag-In a few sites, however, the dispersion innetization. creased with a.f. demagnetization. Samples from 4 sites were then stored for periods of 10, 30 and 100 days after a.f. demagnetization at 125 oersteds and the NRM was measured after each interval of time. Samples from two sites were stored with the +z axis directed downwards, which was the normal way of storage, and the samples from the other two sites were stored with their +z axis directed upwards, i.e., opposite the normal direction of storage. In samples which were stored with the +z axis downward. it was found that in general a component was added in the direction of the earth's field, and in samples stored with the +z axis directed upwards, it was found that in general a component was subtracted in the direction of the earth's field. It was also found that the rate of addition or subtraction of magnetization in the direction of the earth's field decreased with time. The NRM of some samples from these four sites were measured after a storage of 100 days since they were a.f. demagnetized at 125 oersteds, and then they were a.f. demagnetized again. It was found that nearly all of the component added during storage was removed by a.f. demagnetization at 125 oersteds. So it can be assumed that a certain amount of secondary components of magnetization were added to the samples used in this

study, while in storage in the laboratory from the end of summer 1968 until the time of measurement of their NRM, and it can be assumed that these secondary components were removed by a.f. demagnetization at 125 cersteds. The increase in dispersion of directions of NRM of some sites with a.f. demagnetization could be due to the instability of the NRM in samples from these sites. It is also possible that the original NRM was dispersive and thus removal of secondary soft components by a.f. demagnetization contributed to the increase in dispersion.

The average intensity of NRM for the 8 sites from the Unionville granodiorite was 1790 x 10⁻⁶ emu per co before demagnetization and 1320×10^{-6} emu per cc after an a.f. demagnetization at 125 oersteds. The inclination of NRM was 63.6°, and the declination of NRM was 19° before demagnetization, and 65.5°, and 38.9° respectively after demagnetization at 125 oersteds. When the values from two sites of high intensity of NRM were omitted these averages were 910 x 10^{-6} emm per cc for intensity of NRM. 62° for inclination and 12.3° for declination of NRM before demagnetization. and 570 x 10^{-6} emu per cc for intensity of NRM 63.2° for inclination and 39.4° for declination of NRM after demagnetization at 125 oersteds. The average intensity of NRM for samples from 11 sites from the Clancy granodiorite was 580 x 10⁻⁶ emu per co before a.f. demagnetization, and 390×10^{-6} emu per co after demagnetization at 125 cersteds. The average inclination of NRM was 60.1°,

and declination of NRM was 353.9°, before demagnetization, and an inclination of 64.0° and a declination of 347.8° after a.f. demagnetization at 125 cersteds, for 11 sites from the Clancy granodicrite.

The remanent magnetic properties of samples used in this study may not be representative of the remanent magnetic properties of the samples 'in situ'. In situ, secondary soft components of magnetization caused by the earth's present magnetic field may be masked or removed by components derived during sample collection, preparation, and during storage in the laboratory. It is also possible that some of the secondary components of magnetization acquired 'in situ' may have been removed by a.f. demagnetization. Therefore, the measured intensity of remanent magnetization is a minimum in situ value because the NRM and earth's magnetic field have a similar inclination and azimuth. The magnitude of this soft component is unknown, but because it is in the direction of the earth's magnetic field it is considered additive to the magnetic susceptibility, and the resultant of the induced plus the soft component magnetization can be considered as the effective magnetic susceptibility.

CHAPTER VI

MAGNETIC MODELS OF THE NORTHERN MARGIN OF THE BOULDER BATHOLITH

A magnetic profile crossing the northern margin of the Boulder Batholith along a N28.5E azimuth from Prickly Pear valley to the Wickes-Corbin mining area was selected for analysis using the indirect interpretational technique of matching the observed magnetic profile with a calculated profile. The calculated profile is based as much as possible on known geology and measured magnetic properties. The selected magnetic profile is in near proximity to the magnetic property sample sites and a gravity profile quantitatively studied by Renick (1905), and is at right angles to the strike of the magnetic anomaly contours and passes near the crest of the positive magnetic anomaly at the northern margin of the batholith. Renick's observed and calculated profile and associated geological model are shown in Figure 26.

The portion of the U.S. Geological Survey aeromagnetic map (GP-538) from which the magnetic profile is taken is shown in Figure 27a, and the location of the sample sites with respect to the profile is shown in Figure 27b. The earth's normal magnetic field was removed from the magnetic

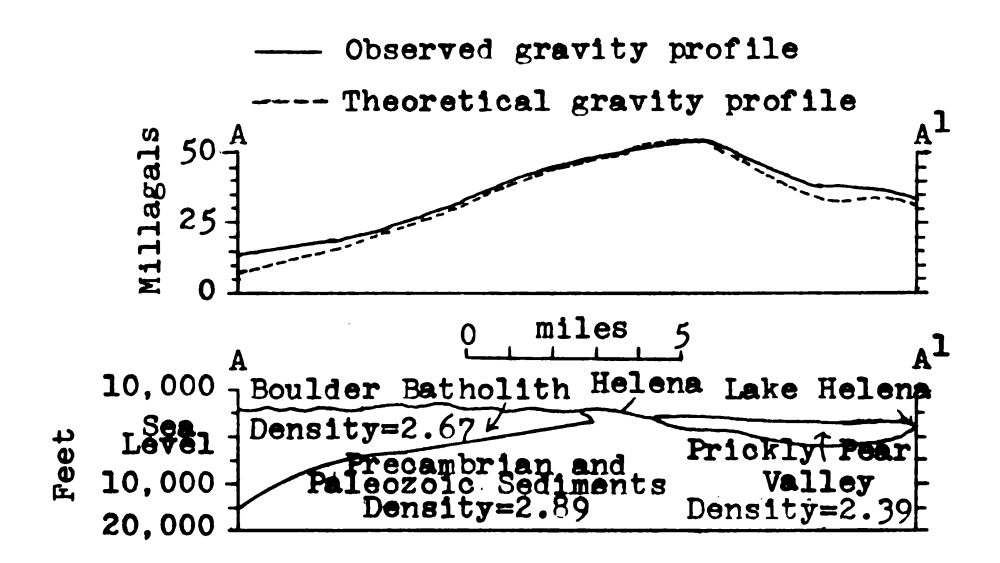


Figure 26. Observed and calculated gravity profile and associated geological model (after Renick, 1965)

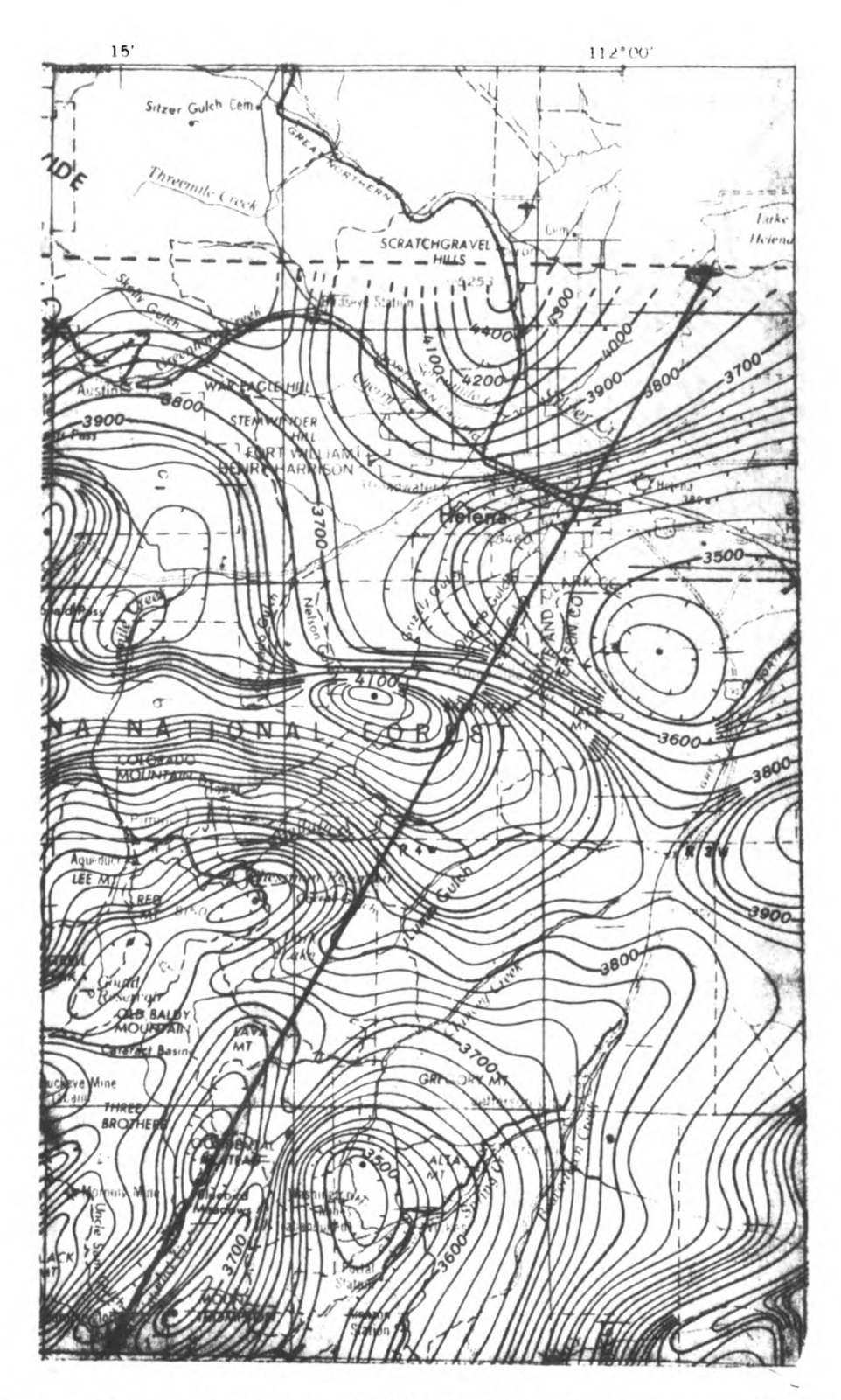


Figure 27a. Portion of the U.S.G.S. aeromagnetic map (GP-538) showing position of analyzed magnetic profile

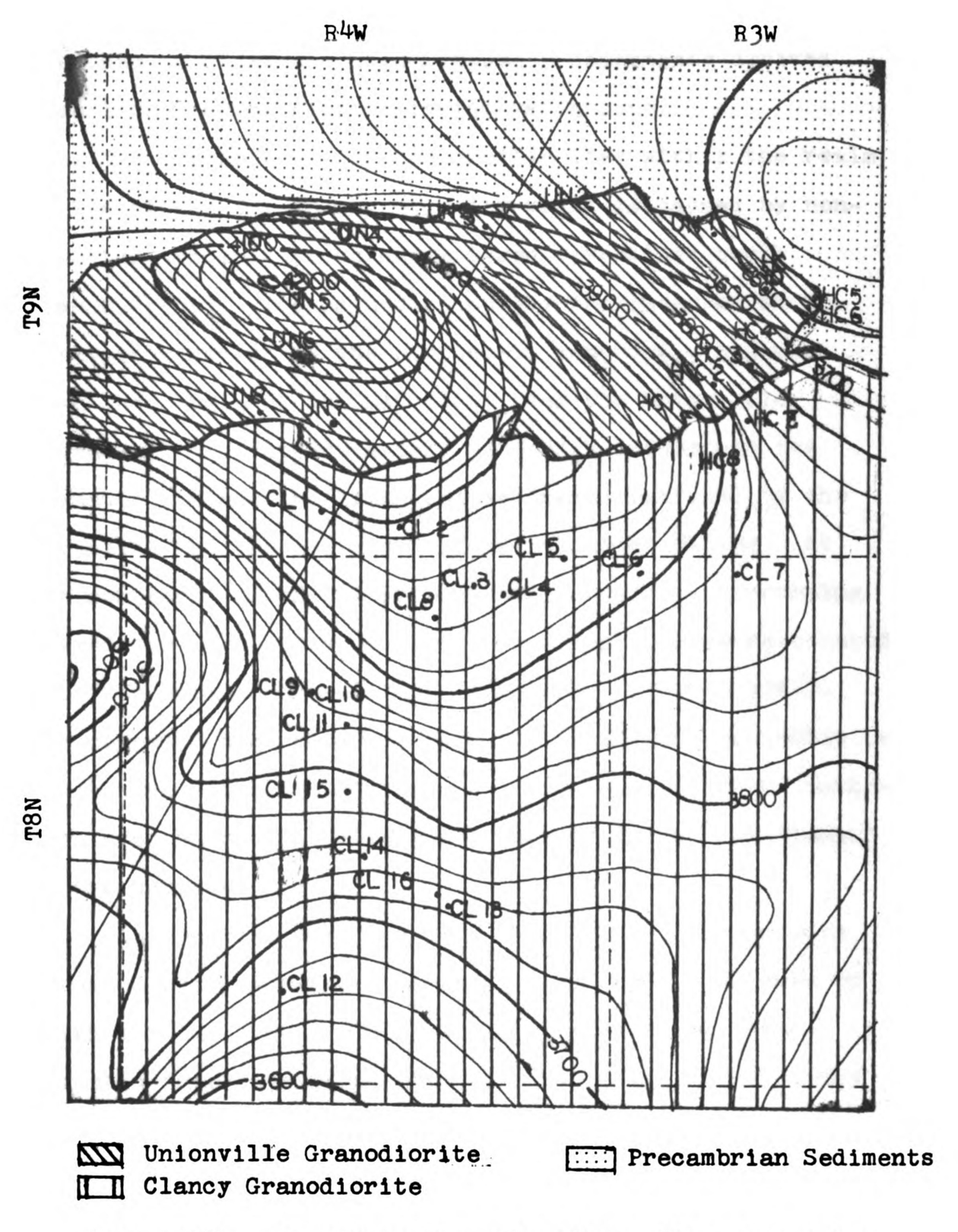


Figure 27b. Location of sample sites with respect to the analyzed magnetic profile

profile assuming a gradient +0.5 per mile to the north, in the direction of N18.5°E, and the profile was hand smoothed to eliminate high frequency components derived from local magnetic polarization variations.

The southern end of the profile lies within the realm of the Wickes-Corbin magnetic low which is caused by nonmagnetic volcanic rocks and altered batholitic rocks (Hanna, 1969). The magnetic anomaly increases at an inconstant gradient to the northeast, reaching a maximum near the margin of the batholith over the Unionville granodiorite of approximately 550% with respect to the magnetic minimum overlying the sediments intruded by the batholith and the sediments of Prickly Pear Walley. At the northern end of the profile the anomaly is increasing toward the north presumably due to igneous rocks associated with the Scratch Gravel Hills (Davis and others, 1963). The magnetic high observed over the Unionville granodiorite is observed discontinuously around the margin of the batholith even where the Unionville granodiorite is not present at the surface.

The magnetic profiles calculated in this study were obtained using a computer program originally developed by Heirztler and others (1962) for determining the total magnetic intensity of two-dimensional bodies of arbitrary cross-section. Calculations were performed using a constant flight elevation of 10,500 feet above sea level, and surface topography smoothed from the U.S. Geological Survey

1:48,000 maps of the area by Knopf (1963), Becraft and others (1963) and Smedes (1964). The Boulder Batholith was treated as two bodies based on the two prominent rock types, the Unionville granodiorite along the margin and the Clancy granodiorite to the south. The margin of the batholith and the contact between the Unionville granodiorite and the Clancy granodiorite along the magnetic profile was taken from the geologic maps of the area by Knopf (1963), Becraft and others (1963) and Smedes (1966). For purposes of calculation the bodies were assumed to strike infinitely perpendicular to the profile and the Clancy granodiorite was extended infinitely to the southwest.

The average magnetic rock properties used in the modeling initially were an average susceptibility of 2730 x 10⁻⁶ emu/cc, and an average intensity of NRM of 1320 x 10⁻⁶ emu/cc, and an inclination of 65.5°, and declination of 38.9° for the Unionville granodiorite. For the Clancy granodiorite an average susceptibility of 2510 x 10⁻⁶ emu/cc and an intensity of NRM of 390 x 10⁻⁶ emu/cc, an inclination of 64.0°, and a declination of 347.8° was used. The remanent magnetic properties are based on the averages from 8 sites from the Unionville granodiorite, and 11 sites from the Clancy granodiorite, which had circles of confidence ~95 of 30° or less. All the values used were obtained after a.f. demagnetization of 125 cersteds. When the values from two sites in the Unionville granodiorite which had an abnormally high intensity of NRM were

eliminated from the calculations, the averages of the Unionville granodiorite were 570×10^{-6} emu/cc for intensity of NRM, and an inclination of 63.2° , and a declination of 39.4° . After a few initial trials to obtain theoretical profiles averages of the 6 sites from the Unionville granodiorite were used, eliminating the abnormally high NRM values.

The samples used in the magnetic property study as stated previously were relatively fresh, unaltered specimens from the batholith. Therefore the results of the susceptibility measurements may not be totally representative because of local alteration which destroys the magnetite and lowers the average magnetic susceptibility. Considering this possibility and the magnetic susceptibility of the intruded rocks, the susceptibility contrasts were assumed to be 2500×10^{-6} emu/cc. for the Unionville granodiorite. and 2000 x 10^{-6} emu/cc for the Clancy granodiorite. The magnetic susceptibility of the intruded sediments is unknown, but should not exceed 100×10^{-6} emu/cc except where local contact metamorphic effects have produced magnetite. For purposes of analysis, the Clancy granodiorite was also divided into eight discrete bodies of decreasing susceptibility with increasing distance from the intrusive contact. The relationship between magnetic susceptibility of the Clancy granodiorite and distance from the contact previously discussed and modification of it were used to determine the susceptibilities.

Initially the magnetic effects of simple geologic models were calculated assuming vertical, and 45° SW dipping contacts extending to depths of 5, 8, 10, 12, and 15 km for both induced, and induced plus remanent magnetization. None of the calculated profiles matched the observed profile, and a study of these profiles revealed that varying the depth to the bottom changed the anomaly only slightly, thus in subsequent models the bottom of the batholith was placed at 10 km below sea level following the results of Burfeind (1967) and Biehler and Bonini (1969).

The geologic model of the northern margin of the batholith derived by Renick (1965) from gravity was used as the basis of a variety of magnetic models calculations. Renick's model (Figure 26) has the contact of the batholith dipping 45° to the northeast from the surface to a depth of 3,500 feet above sea level, where the dip then reverses to 68° southwest. The total magnetic intensity anomalies of four different magnetic models based on Renick's model and the measured magnetic properties are shown in Figures 28 and 29.

In Figure 28 profile 1 was obtained with the Clancy granodiorite assumed to be a single body, with the contact between the Clancy and Unionville granodiorite extending to the bottom of the batholith. Profile 2, in Figure 28, was obtained for a similar model but the Clancy granodiorite was divided into eight bodies, each with decreasing susceptibility with distance from the intrusive contact. In

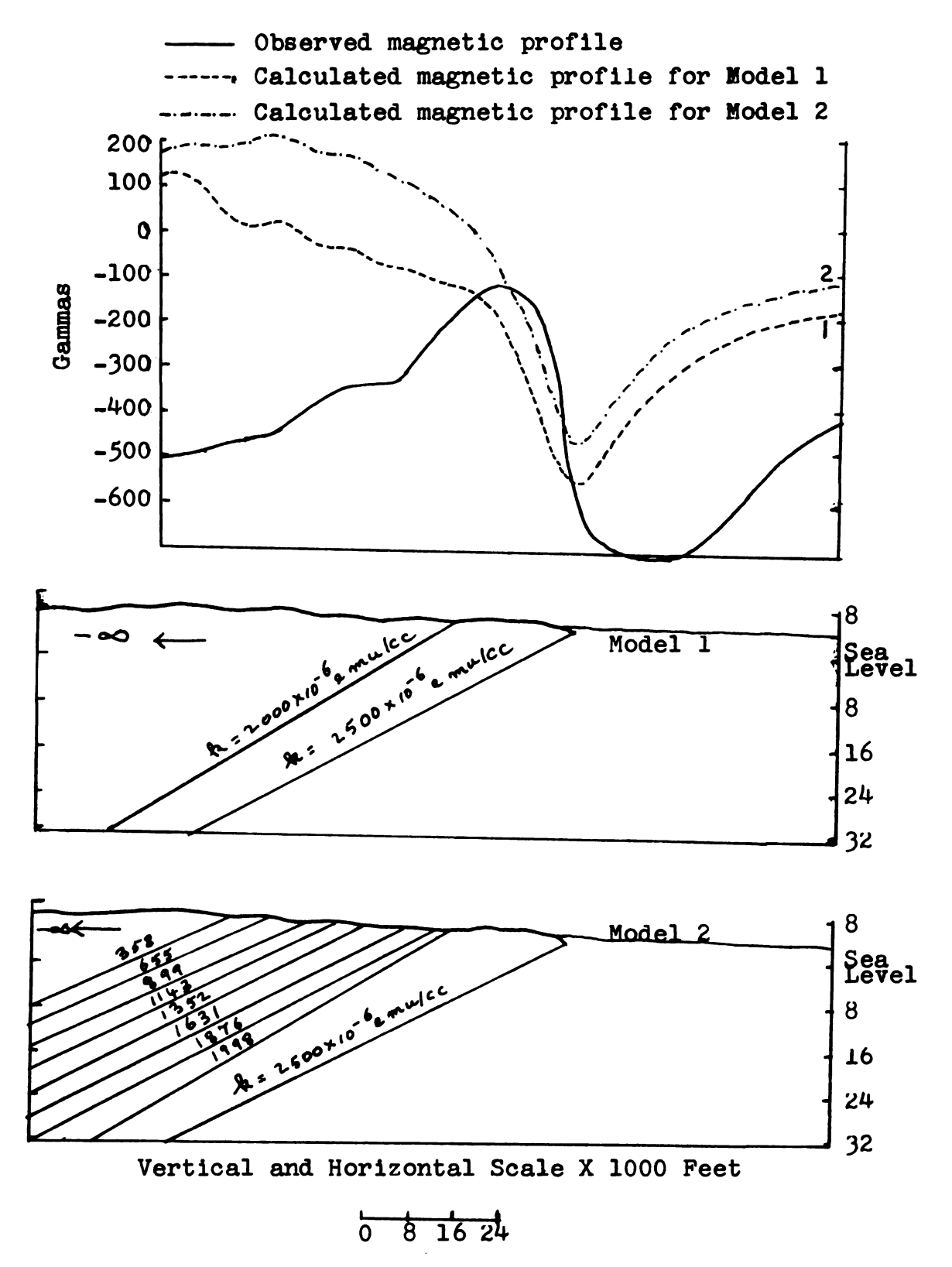
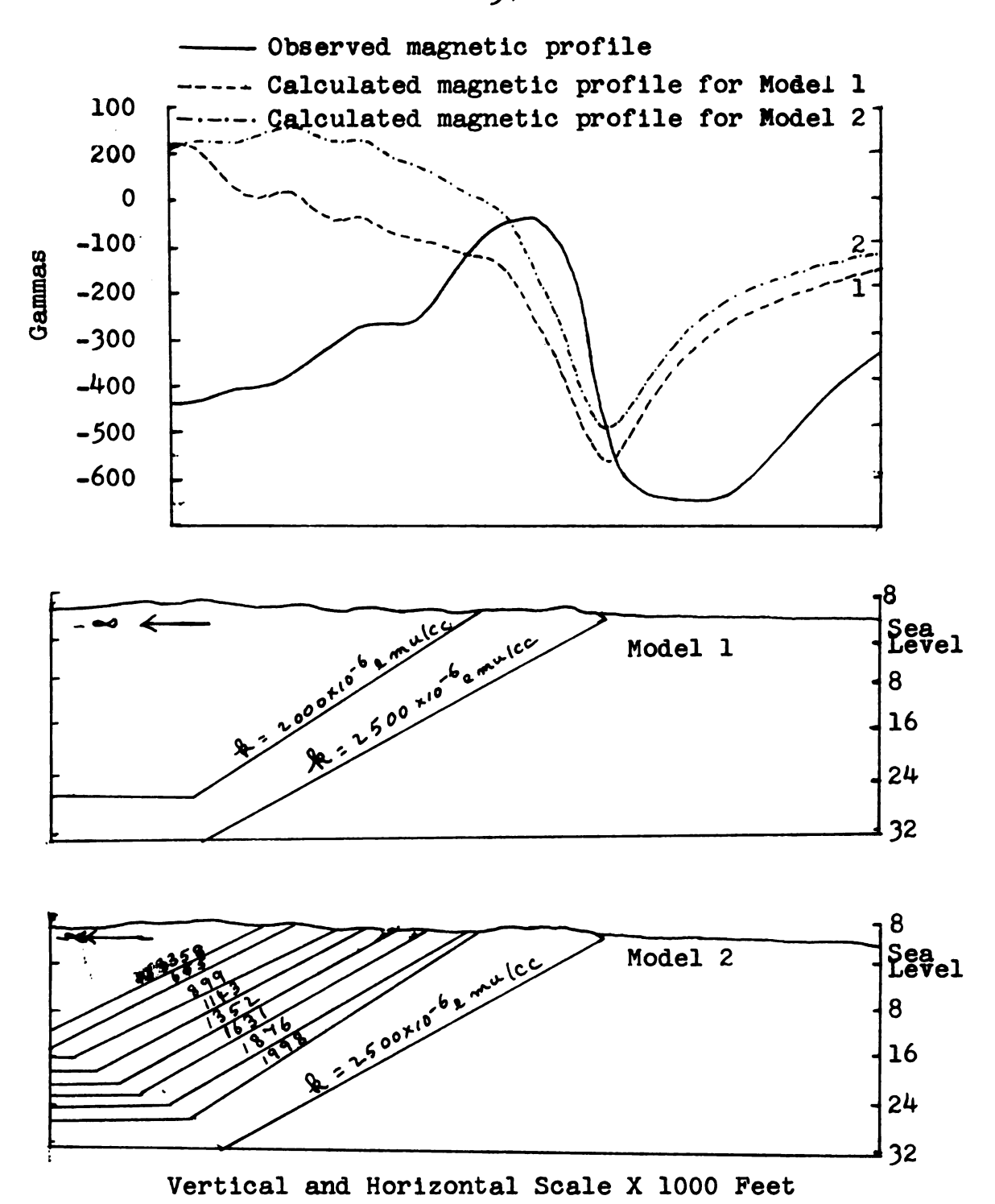


Figure 28. Calculated and observed profiles and associated magnetic models derived from gravity studies

Figure 29 profile 1 was obtained with the Unionville granodiorite extending horizontally to an infinite distance to
the south below the Clancy granodiorite. Profile 2 in Figure
29 was obtained with the Clancy granodiorite divided into 8
discrete bodies, each with decreasing susceptibility with
distance from the intrusive contact and with each body
overlying the body to the northwest. As can be seen in
Figures 28 and 29, these body configurations do not produce
the observed anomaly.

Renick's (1965) geologic model had to be modified to account for the observed anomaly. A body with vertical contacts to the bottom after dipping at an angle of 45° to the northeast from the surface to a depth of 2.6 km was Profiles calculated using this basic configuraassumed. tion matched reasonably well with the observed profile. The match was good over the contact between the batholith and the sediments. however the anomaly at the southern end of the calculated profile was higher than in the observed profile, and the anomaly at the northern end of the profile was lower than in the observed profile. The poor match of the southern end of the calculated profile with the southern end of the observed profile could be due to the Wickes-Corbin magnetic low being superimposed on the anomaly of interest, and the net effect would be a low on the southern end of the observed profile. The poor match of the northern end of the calculated profile with the observed profile could be due to the anomaly associated



0 8 16 24

Figure 29. Calculated and observed profiles and associated magnetic models based on gravity derived model

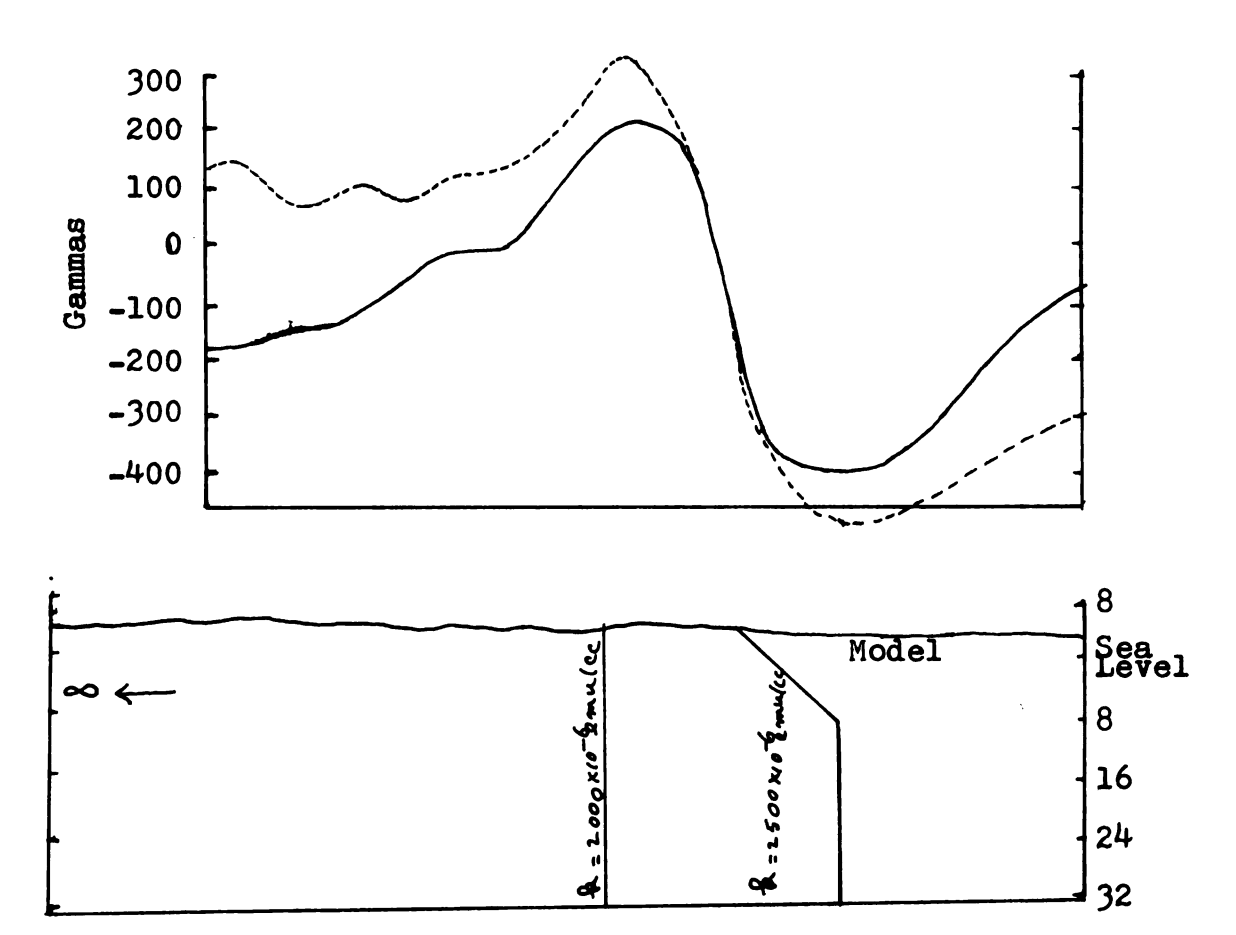
with igneous rocks of the Scratch Gravel Hills being superimposed over the anomaly of interest in the study. The
effect of the igneous rocks of the Scratch Gravel Hills
in the north, and the Wickes-Corbin area in the south were
not considered in calculating theoretical profiles and,
therefore, a poor match of the calculated and observed
profiles on the north and south ends of the profiles is
not unexpected.

The calculated profiles with the associated models are shown in Figures 30a and 30b. The calculated profile in Figure 30a is obtained with the Clancy granodiorite as a single body and the calculated profile in Figure 30b was obtained by dividing the Clancy granodiorite into eight bodies each with decreasing susceptibility with distance from the intrusive contact.

Profiles calculated with these body configurations, but assuming induced magnetization only, and induced only and induced plus remanent magnetization with a dip of 45° southwest did not match the observed profile.

The geologic models shown in Figure 30, which result in magnetic anomalies that match the observed magnetic anomaly reasonably well do not represent unique solutions. However, in view of the geologic and magnetic property control, they can be considered good approximations to the actual geologic situation. This conclusion is perplexing in view of the considerably different geologic model derived from gravity study, particularly because the gravity

Observed magnetic profile
--- Calculated magnetic profile for Model



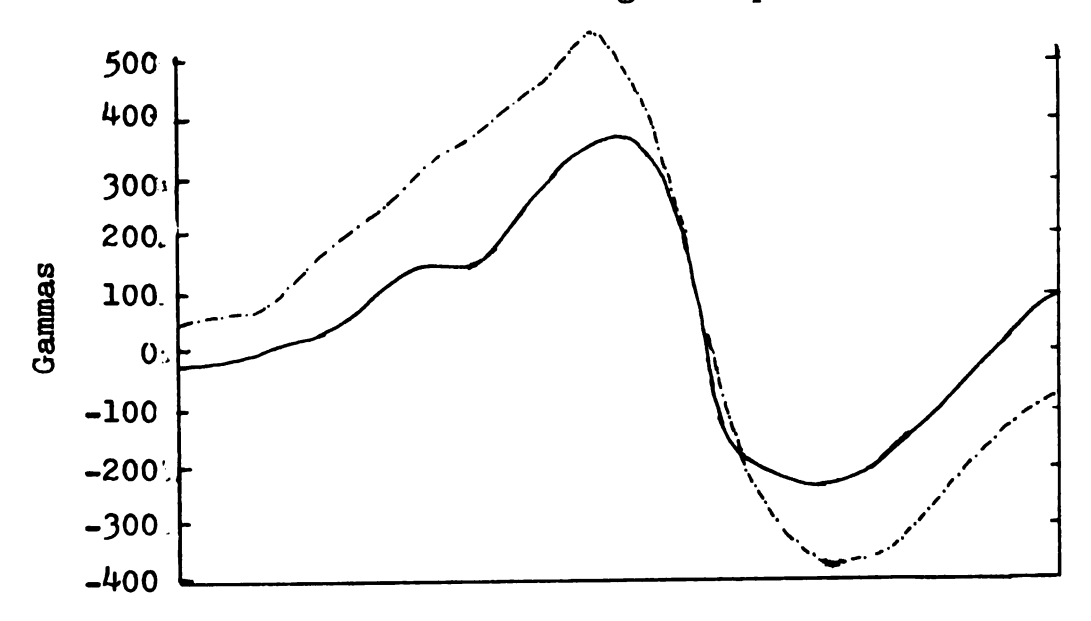
Vertical and Horizontal Scale X 1000 Feet

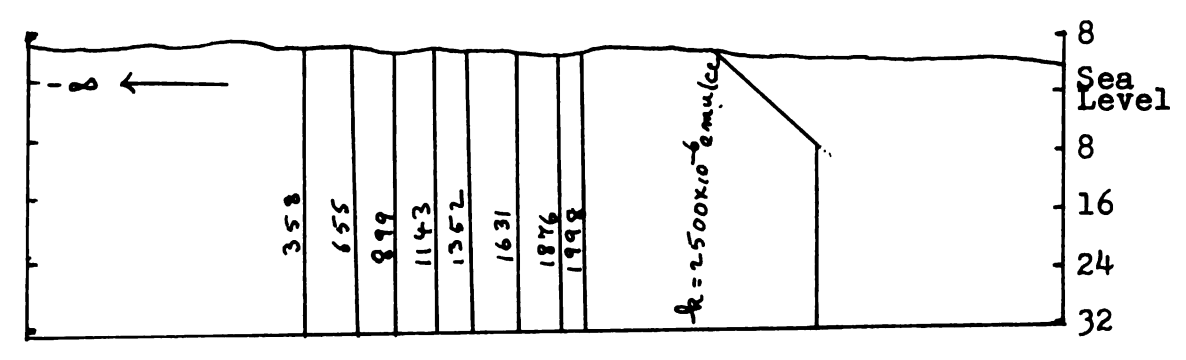
0 8 16 24

Figure 30a. Calculated magnetic profiles and associated magnetic models which approximate the observed magnetic profile: Clancy granodiorite assumed to be a single body

---- Observed magnetic profile

----- Calculated magnetic profile for Model





Vertical and Horizontal Scale X 1000 Feet

0 8 16 24

Figure 30b. Calculated magnetic profiles and associated magnetic models which approximate the observed magnetic profile: Clancy granodiorite divided into 8 discrete bodies

method is usually superior to the magnetic method in quantitative structural analysis. The differences between these two models can be resolved by considering the densities Renick (1965) used in his calculations. Using rock densities measured by Kinoshita and others (1963) he assigned a density of 2.67 g/cc to all the batholith rocks and 2.89 to the intruded sediments. However Knopf (1963) has found that the Unionville and Clancy granodiorites at the north end of the batholith have average densities of 2.78 and 2.71 g/cc respectively. The density of the rocks intruded by the Boulder Batholith probably average about 2.81 g/cc and Knopf (1963) has found that the Precambrian Selt sedimentary rocks at the north end of the batholith have a density range from 2.71 to 2.78 g/cc. Thus the Unionville granodiorite may have no density contrast or at most only a few hundredths of gram per cubic centimeter contrast with the intruded rocks. As a result a gravity model calculated without considering these findings would show the batholith shifted to the south, or dipping to the south as Renick has done. Therefore, the geologic models derived from the magnetic analysis should be considered closer to the actual situation than the model derived from the gravity study.

CHAPTER VII

SUMMARY

Magnetic properties of surface core samples from 33 sites in the northern margin of the Boulder Batholith, near Helena, Montana, have been measured and a geologic model for the northern margin of the batholith is obtained from the magnetic properties, surface geology, and a magnetic profile.

Fifteen of the 33 sites are from the marginal Union-ville granodiorite, and the remaining sites are from the interior Clancy granodiorite. Each site had 5 to 8 samples. The intensity and directions of NRM of the samples were measured using a spinner magnetometer, and the magnetic susceptibility of these samples was measured using a susceptibility bridge. All the samples were a.f. demagnetized to remove the secondary components of magnetization which may have been acquired by the samples while they were being drilled and cut to size, and during storage in the laboratory. Samples from 17 sites were demagnetized at levels of 50, 125, 250 and 400 cersteds. On the basis of the results obtained by a.f. demagnetizing samples from these 17 sites, the samples from the remaining 16 sites were a.f. demagnetized at only 125 cersteds.

Fisher's parameters were calculated for all the sites. Sites which had a circle of confidence (<95) of less than 30° were arbitrarily excluded from the calculation of the rock type averages. Eight sites from the Unionville granodiorite and ll sites from the Clancy granodiorite have circles of confidence <95 of 30° or less. Two of the 8 sites from the Unionville granodiorite had high intensities of NRM, and so they were excluded from the calculation of the averages for the rock type. Average values for these sites after a.f. demagnetization of 125 cersteds were used in modeling studies.

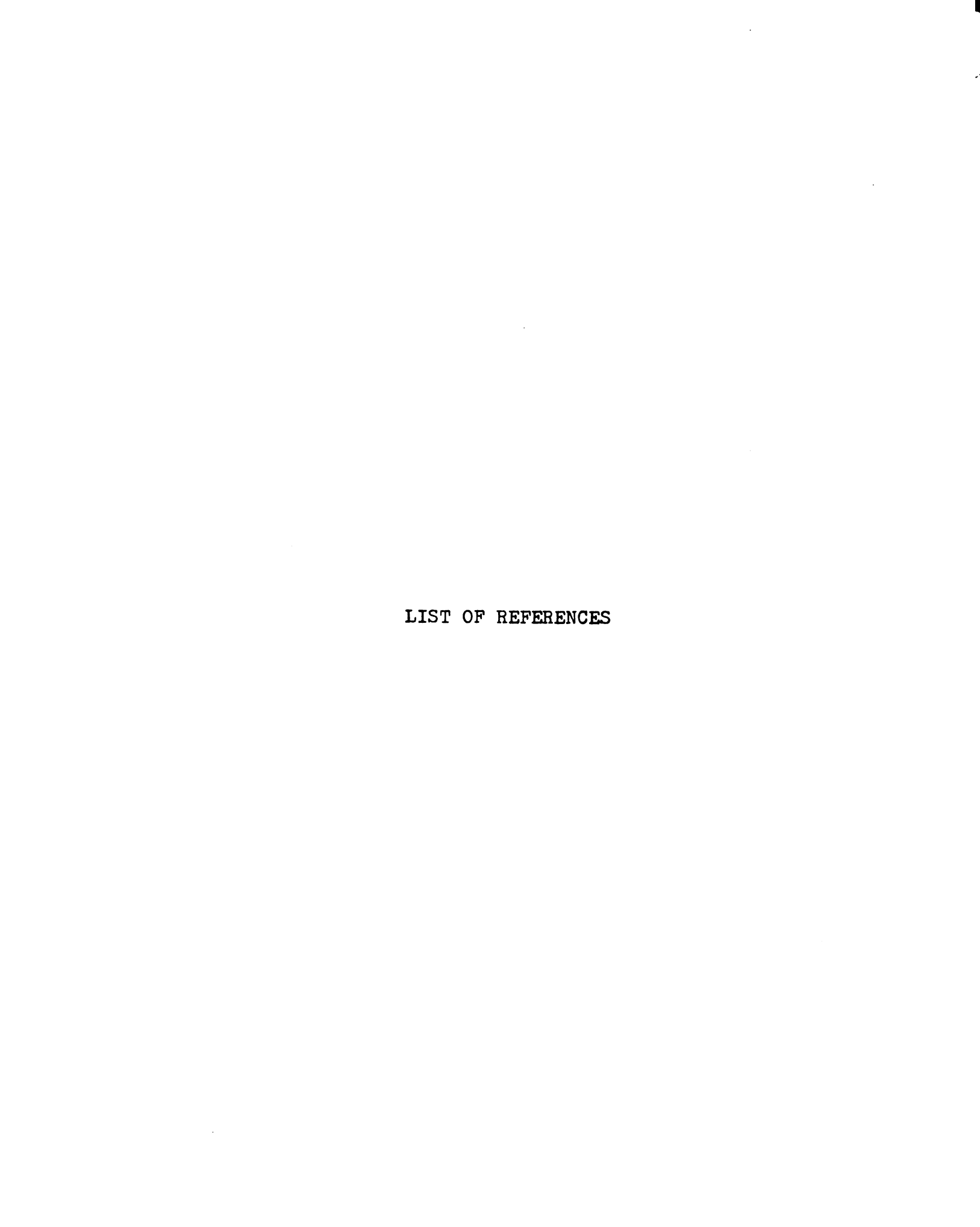
The samples from Unionville granodiorite had an average intensity of NRM of 570×10^{-6} emu per cc, and an inclination of 63.2° , and a declination of 39.4° , after a.f. demagnetization at 125 oersteds. The samples from the Clancy granodiorite had an average intensity of NRM of 390×10^{-6} emu per cc, an inclination of 64.0° , and a declination of 347.8° after demagnetization at 125 oersteds.

The samples from the Unionville granodiorite had an average magnetic susceptibility of 2730×10^{-6} emu per cc, and the samples from the Clancy granodiorite had an average susceptibility of 2510×10^{-6} emu per cc. It was found that a linear relationship exists between the distance of a site in the Clancy granodiorite from the northern margin of the batholith and the susceptibility of a site. The susceptibility of a site in the Clancy granodiorite decreases with distance from the contact. The samples used in this study

are relatively fresh unaltered samples from the batholith and thus they may not be representative of the batholith. Therefore, in the final model studies, an average magnetic susceptibility of 2500×10^{-6} emu per cc was assigned to the Unionville granodiorite, and a value of 2000×10^{-6} emu per cc was assigned to the Clancy granodiorite. The Clancy granodiorite also was divided into 8 discrete bodies each with decreasing susceptibility with distance from the intrusive contact using a modified linear relationship.

A magnetic profile from U.S. Geological Survey GP 538 was selected for analysis of the two major rock units in the Boulder Batholith on the basis of the rock magnetic properties obtained in this study, and to develop a model to outline the depth extent, and configuration of the batholith. The profile has a direction of N28.5°E, and extends from Prickly Pear Valley in the north to the Wickes-Corbin area in the south and crosses the northern margin of the batholith.

The model proposed in this study for the northern margin of the Boulder Batholith, has vertical contacts to a depth of 10 km, after dipping at an angle of 45° to the northeast from the surface to a depth of 2.6 km. This model differs from a model previously derived from a gravity study. The difference is explained in terms of the density values used in deriving a model based on gravity data.



LIST OF REFERENCES

- Becraft, G. E., Pickney, D. M., and Rosenblum, S., 1963.
 "Geology and mineral deposits of the Jefferson City
 quadrangle, Jefferson and Lewis and Clark counties,
 Montana," USGS, Professional Paper 428.
- Biehler, S., and Bonini, W. E., 1969. "A regional gravity study of the Boulder Batholith, Montana," Geological Society of America, Memoir 115, pp. 401-422.
- Burfeind, W. I., 1967. "A gravity investigation of the Tobacco root mountains, and Jefferson basin, Boulder Batholith and adjacent areas of southwestern Montana," unpublished Ph.D. thesis, University of Indiana.
- Davis, W. E., Kinoshita, W. T., and Smedes, H. W., 1963.
 Bouguer gravity, aeromagnetic and generalised geologic survey of East Helena, and Canyon Ferry quadrangles and part of the Diamond city quadrange, Lewis and Clark, Broadwater and Jefferson Counties, Montana, U.S.G.S. Geophys. Inv. Map GP-444.
- Davis, W. E., Kinoshita, W. T., and Robinson, G. D., 1965a.
 Bouguer gravity, aeromagnetic, and generalized geologic map of the western part of the Three Forks Basin,
 Jefferson, Broadwater, Madison, and Gallatin Counties,
 Montana, U.S.G.S. Geophys, Inv. Map GP-497.
- Davis, W. E., Kinoshita, W. T., and Robinson, G. D., 1965b, Bouguer gravity, aeromagnetic, and generalized geologic map of the eastern part of the Three Forks Basin, Broadwater, Madison, and Gallatin Counties, Montana, U.S.G.S. Geophys. Inv. Map GP-498.
- Doell, R. R. and Cox, A., 1965. "Measurement of the remanent magnetization of igneous rocks," U.S. Geological Survey Bull. 1203-A.
- Doell, R. R., and Cox, A., 1967. "Analysis of alternating-field demagnetization equipment, in <u>Methods in Paleo-magnetism</u>," edited by K. M. Creer, D. W. Collinson, and S. K. Runcorn, Elsevier Publishing Co., Amsterdam.

- Fisher, R. A., 1953. "Dispersion on a sphere," Proceedings of the Royal Society (London) Series A 217: 295-305.
- Hanna, W. F., 1969. "Negative aeromagnetic anomalies over mineralised areas of the Boulder batholith, Montana," Geological Survey Research, 1969.
- Hanna, W. F., 1967. "Paleomagnetism of upper cretaceous volcanic rocks of southwestern Montana," Journal of Geophysical Research, Vol. 72, No. 2, pp. 595-610.
- Heirtzler, J. R., Peter, G., Talwani, M., and Zurfluch, E. G., 1962. Magnetic Anomalies caused by Two-Dimensional Structure: Their computation by Digital computers and Their interpretation, Lamont Geological Observatory Technical Report Number 6.
- Johnson, R. W., Jr., Henderson, J. R., and Tyson, N. S., 1965. Aeromagnetic map of the Boulder batholith area, southwestern Montana. U.S.G.S. Geophys. Inv. Map GP-538, Scale 1:250,000.
- Kinoshita, W. T., Davis, W. E., and Robinson, G. D., 1964a. Aeromagnetic, Bouguer gravity and generalized geologic map of Toston and Radersburg quadrangles and part of the Devils Fence quadrangle, Gallatin, Broadwater, and Jefferson Counties, Montana, U.S.G.S. Geophys. Inv. Map GP-496.
- Kinoshita, W. T., Davis, W. E., Smedes, H. W., and Nelson, W. H., 1964b. Bouguer gravity, aeromagnetic, and generalized geologic map of Townsend and Duck Creek Pass Quadrangles, Broadwater County, Montana, U.S.G.S., Geophys. Inv. Map GP-439.
- Knopf, A., 1963. "Geology of the northern part of the Boulder Bathylith and adjacent area, Montana." U.S.G.S. Misc. Geol. Inv. Map 1-381, Scale 1:48.000.
- Knopf, A., 1957. "The Boulder Bathylith of Montana," American Journal of Science, Vol. 255, No. 2, pp. 81 to 103.
- Klepper, M. R., 1962. "Emplacement of the Boulder batholith," Address to the Rocky Mountain Minerals Conference, A.I.M.E., Butte, Montana.
- MacClure, T. W., 1970. "The development of a functional magnetometer for measurement of remanent magnetisation," unpublished M.S. thesis, Michigan State University.
- Renick, H. Jr. "A gravity survey of the Boulder batholith and Prickly Pear valley near Helena, Montana", Compass, Vol. 42, No. 4, pp. 217-244.

- Smedes, H. W., 1966. "Geology and igneous petrology of the northern Elkhorn mountains, Jefferson and Broadwater counties, Montana," U.S.G.S. Professional Paper 510.
- Tilling, R. S., Klepper, M. R., and Obradovich, J. D., 1968.
 "K-Ar ages and time span of emplacement of the Boulder batholith Montana," American Journal of Science,
 Vol. 266, October 1968, pp. 671-689.

MICHIGAN STATE UNIV. LIBRARIES
31293104745447